Introduction of perovskite based materials: Synthesis, properties, and applications

Highlights

This chapter provides a brief description of research background and the motivation behind the current investigation along with a brief literature review on perovskite materials. Perovskite materials are briefly described, along with their many classifications and attributes. Several synthetic routes of perovskites nanocomposites with their potential applications as sensor materials are emphasized. The chapter concludes with a discussion of the objectives and plan of the present study.

1.1. Motivation and background

Metal halide perovskites (MHPs) are rapidly emerging as one of the most promising materials of the twenty-first century. They offer a variety of fascinating features and have significant potential for a wide range of applications, including photovoltaics (PV), optoelectronics, photocatalysis, among others. Lead halide perovskites (LHPs) have drawn massive attention in PV applications owing to their unique electrical and optical properties such as direct band gap, long exciton diffusion lengths, high absorption coefficient and high charge carrier mobility [1-3]. The earlier successes of colloidal conventional semiconductor quantum dots (QDs) e.g. CdSe, CdTe, PbS, PbSe, InP, etc. paved the way for the study of MHPs in the form of perovskite QDs. In the recent years, perovskite nano crystals (PeNCs) have emerged as peerless optoelectronic materials because of their outstanding optical properties [4]. Hybrid $CH_3NH_3PbX_3$ and all inorganic $CsPbX_3$ PeNCs have prompted extensive research efforts because of their ease of synthesis, highly intense and narrow emission colors, solution processibility, very high photo luminescence quantum yield (PLQY), as well as tunable emission and absorption over the entire visible spectrum, etc. These unique properties of PeNCs make them a promising fluorescent material among the family of conventional nano materials and find potential applications in lighting and display technology. Also, it could be an ideal candidate for sensing applications. Very recently several research groups have utilized the tunable optical features of PeNCs for the sensing of various target analytes [5,6]. The PeNCs based sensing techniques have the benefit of being highly selective and highly responsive to the target analytes. Thus, perovskite nanoparticles may create new analytical avenues for the detection of a wide range of chemical species.

1.1.1. A brief history of Perovskite based material

Metal halide Perovskite materials, which offer a number of intriguing characteristics and enormous potential for a variety of applications, have recently attracted significant scientific interest. The first perovskite, calcium titanate ($CaTiO_3$) is a representation of perovskite minerals in their native state which was initially discovered in the Ural Mountains in 1839 by German mineralogist Gustav Rose of the University of Berlin. He gave this substance Lev Perovski's (1792–1856) name, a Russian mineralogist [7]. Following that, multiple research efforts were directed towards the development of various oxide based perovskites with appealing ferroelectric, magnetic, thermoelectric, and superconductive properties [7-10]. After 119 years, since the discovery of oxide based

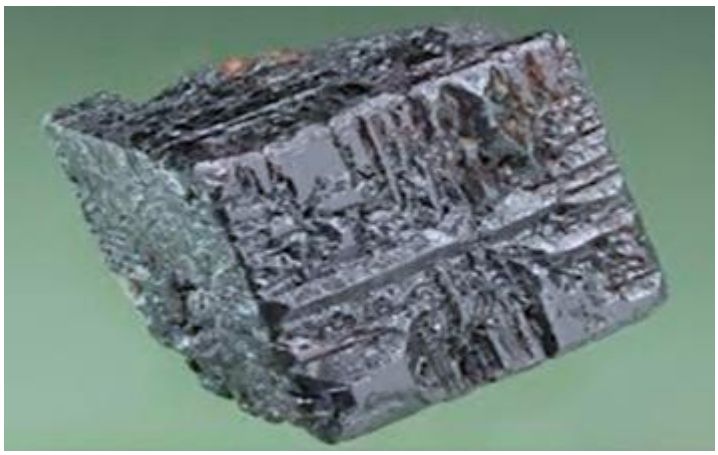

Figure 1.1: Structure of $CaTiO_3$ perovskite mineral [13]

perovskites, Moller and his group disclosed the first halide-based perovskite cesium lead halide ($CsPbX_3$) structure in 1958 [11]. Although bulk $CsPbX_3$ perovskites were first reported in 1893, but their important properties e.g. crystal structure, photoconductive and semiconducting properties were not explored. Several lead-free halide perovskites, including $CsSnX_3$ and $CsGeCl_3$, were also investigated at that time [4,12]. Weber et al. synthesized and identified the crystal structure of organic inorganic hybrid halide perovskite, methylammonium lead halide ($MAPbX_3$) in 1978 [14]. Their prospective uses in optoelectronics drew attention in early 2000s. MHPs were first used in solar cells by Kojima et al. in 2009 as light sensitizers, but it required further 3 years to realize their full potential for efficient photovoltaics [15]. Since then, numerous research efforts have been conducted to increase the potential of this material in photovoltaics and surpassed the power conversion efficiency within a short period of time. Then the research interest of MHPs shifted from bulk material to perovskite nanocrystals. In the year of 2015, Protesescu's research team for the 1st time prepared $CsPbX_3$ (X= Br, Cl, I) PeNCs and explore its optoelectronic properties. They synthesized the nanocrystals (NCs) by modifying the hot injection method, having size distribution in the range of 4-15 nm with tunable band gap covering the visible spectrum of 410-700 nm [16]. Following this research several reports have been introduced the highly luminescent PeNCs for wide range of applications including solar cells, lighting and display technology, photodetector and very recently in sensing applications.

1.2. Classification of Perovskite Materials

Perovskites are categorized into different classes on the basis of their composition, dimensionality, stoichiometry, and crystal structure.

1.2.1. Composition based Classification

Perovskites are classified as inorganic oxide perovskites, alkaline metal halide perovskites and organic-inorganic halide perovskites on the basis of A cation and the X anion of ABX_3 perovskites (Figure 1.2).

1.2.1.1. Inorganic Oxide based Perovskites: Oxide perovskites with ABO_3 formula are generated by combining a divalent metal cation (Ca^{2+}, Mg^{2+}, Sr^{2+}, Ba^{2+}, etc.) and a tetravalent M^{4+} (Ti^{4+}, Si^{4+}, Sn^{4+}, Fe^{4+}) with O act as the anion. In the typical crystal structure of ABO_3, the smaller B cation is bonded with six oxygen atoms through ionic bonds to form BO_6 octahedra. The larger A cation coordinated with the 12 adjacent O atom in the ideal cubic symmetrical structure. They are generally colorless and have wide band gap in the range 3–5 eV [17]. By adjusting the composition of oxide perovskites, a wide range of electronic properties including capacitive, superconductive, catalytic, metallic, and magnetic properties are achieved. Therefore, doping of the oxide perovskites with other metal ions has improved their electrical and magnetic properties. Perovskite oxides enable nearly unlimited compositions with special features by allowing fractionally doping various metals in both the A and B sites and generating crystal structures with about 15 symmetries that have been proven to have vast uses. $LaAlO_3$ doped with Mn and Sr was the first perovskite oxide to be experimentally proven to effectively split CO_2 and water to form carbon monoxide and hydrogen [18].

1.2.1.2. Halide Perovskites: In halide based perovskites, the oxygen in the formula ABO_3 is replaced with X anion (X = Cl, Br, I). Lead halide perovskite materials have drawn massive attention in photovoltaics owing to their unique properties such as direct band gap, longer exciton diffusion lengths, high absorption coefficient and high charge carrier mobility. Also, their remarkable optoelectronic properties including very high PLQY, narrow and intense emission line, tunable emission wavelength etc., make them a promising luminescent material for variety of applications. They can be further classified into two types based on the nature of A cation-

(a) All inorganic halide perovskite materials

(b) Organic-inorganic hybrid halide perovskite materials

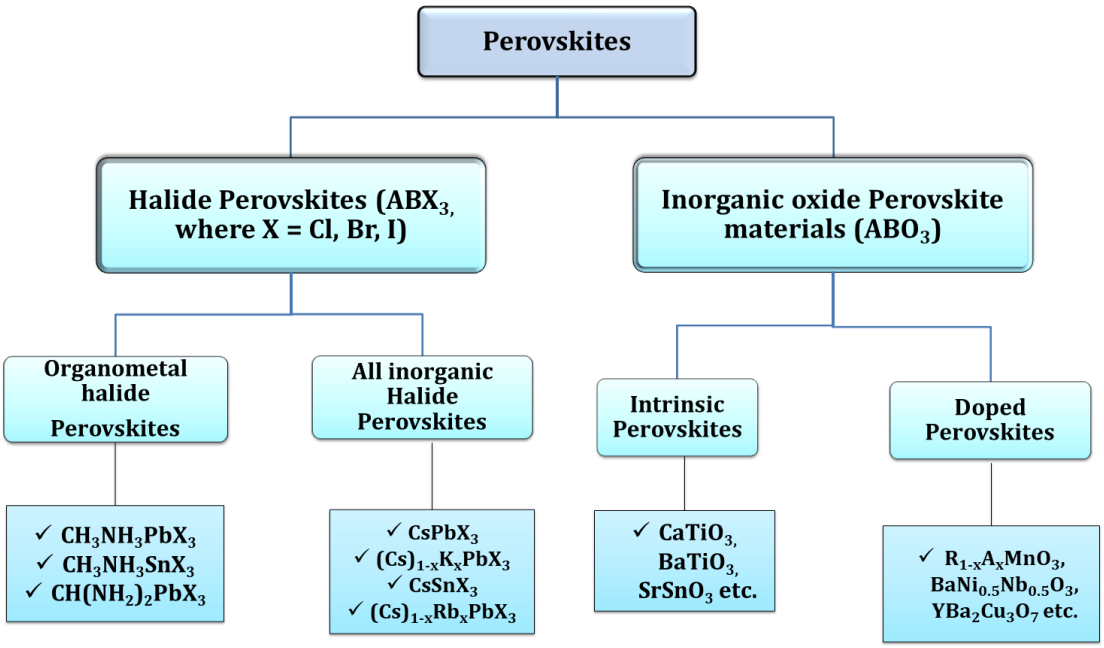

Figure 1.2: Classification of perovskite materials according to their composition & stoichiometry.

(a) All inorganic halide perovskite materials: Inorganic halide perovskites are formed when an inorganic metal ion such as cesium (Cs) or rubidium (Rb) acts as monovalent A site cation. In terms of stability, inorganic perovskites are great alternatives of organic-inorganic hybrid perovskite as they replace the volatile organic cation with stable inorganic ions. Inorganic halide perovskites such as $CsPbI_3$, $CsPb(Br/Cl)_3$, $CsPbBr_3$, $CsSnI_3$, and $CsPbI_{3-x}Br_x$ are well known for producing perovskite quantum dots [19,20].

(b) Organic-inorganic hybrid halide perovskites: When the A site cation of ABX_3 refers to organic cation such as methylammonium ($CH_3NH_3^+$), formamidinium ($CH(NH_2)_2^+$), dimethylammonium ($(CH_3)_2NH_2^+$) with B cation of Pb^{2+}, Sn^{2+}, and Ge^{2+}, it is termed as organic-inorganic hybrid perovskite materials. Such perovskites also exhibit excellent optical and electrical properties. However, being a volatile organic component with a weak H-bond between the organic cation and lead halide, it degrades easily when exposed to extreme environmental conditions [21,22].

1.3. Crystal structure and general properties of Perovskites

Perovskite materials exhibit eye catching structural, optical and electronic properties, making them a recent wonder material for wide range of applications. PeNCs have drawn enormous attention in recent years due to their prominent effects on the electronic and

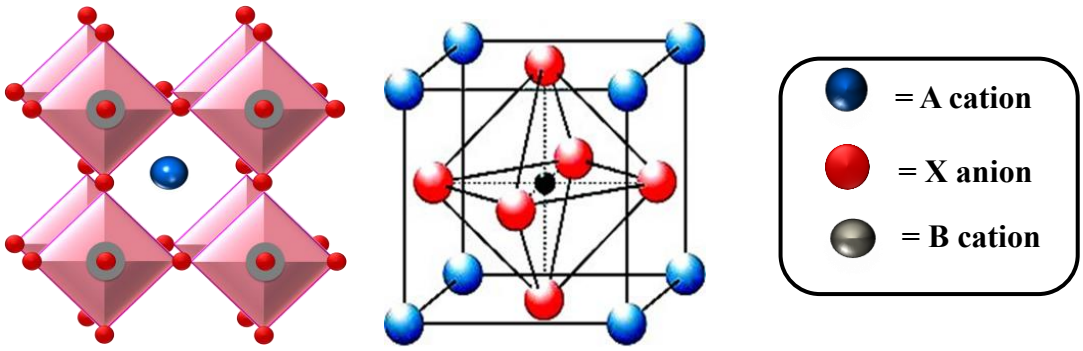

Figure 1.3: Crystal structure of ABX_3 type perovskite material.

photoelectronic properties. Here, we have discussed the properties of perovskites by considering all inorganic halide perovskites.

1.3.1. Crystal structure

The common chemical formula for the perovskite lattice structure is ABX_3 (A = inorganic or organic cation; B = Pb, Sn, Ge etc. and X = halide or oxide ion), where A being the larger cation than B with 12-fold coordination with X. The B metal cation is encircled by six "X" to form a BX_6 octahedra. The ideal cubic perovskite structure is best visualized in terms of the BX_6 octahedra, which are corner connected and the A cation occupies the hole created by BX_6 octahedral, forming a three dimensional network (Figure 1.3). The structure and phase stability of perovskites are mostly dependent on the octahedral factor and Goldschmidt's tolerance factor (t) which gives the correlation between the radii of A (R_A), B (R_b) and X (R_x) [23,24]. Tolerance factor was represented by the equation,

$$t = \frac{(R_A + R_X)}{\sqrt{2}(R_B + R_X)} \qquad (1.1)$$

and octahedral factor, $\mu = \frac{R_B}{R_X}$ (1.2)

To form an ideal cubic perovskite lattice, the value of t seems to be extremely close to 1. The inorganic halide perovskites have t and μ value lies in $0.8 \leq t \leq 1$ and $0.44 \leq \mu \leq 0.9$. On dropping or surpassing the t value from the upper limit may allow the perovskite to transition into a non-perovskite phase as a result of lattice distortion [25]. The B-X-B bond angle can be adjusted, widely thanks to the hinged octahedra, and the symmetry is reduced to multiple tilt transitions, which are sets of cooperative rotations of the BX_6 octahedra. A slight distortion in the PbX_6 octahedral cage of lead halide perovskites can change the crystal phase from tetragonal to cubic one with change in temperature. There is a remarkable structural tunability from 3D to lower dimension based upon corner shared

BX_6 octahedra [26,27]. Different crystal forms for inorganic perovskites can be achieved through interactions between these A, B, and X ions.

1.3.2. Electrical Properties

The electronic characteristics of MHPs are mainly influenced by BX_6 segment of the perovskite. The A cation have least contribution in electronic properties. Therefore, MHPs with both the MA^+ and Cs^+ have similar electrical properties around band edge level. Chang et al. in 2004 first investigated the electronic structure of $CsPbX_3$ and $MAPbX_3$ using first principle pseudopotential calculations. They came with the conclusion that the band edge states for both perovskites are mostly derived from the Pb-X bond of PbX_6 octahedra and the electronic bands originating from the organic cation are located deep inside the valence band (VB) and conduction band (CB). Additionally, band gaps of the perovskites are found to be red shifted with pressure that results from the pressure sensitive antibonding and nonbonding properties of the valence band maxima (VBM) and conduction band maxima (CBM) [28,29]. MHPs exhibit excellent charge carrier properties due to the ambipolar charge carrier migration and lower exciton binding energies. Moreover, they have tolerance capacity to defects, resulting into longer carrier lifetime and carrier diffusion length [4,30]. Due to all these fascinating electrical properties, MHPs find promising applications in the field of optoelectronics and flexible electronics.

1.3.3. Optical Properties

MHPs have significant optical absorption and a tunable band gap. Researchers found that when perovskites are synthesized in the form of perovskite nanocrystals, they display exceptional optical qualities and significantly better brightness and a narrower emission line with very high PLQY value than other conventional QDs (CdS, CdSe, InP, CDs, etc.) [31,32].

1.3.3.1. Absorption feature

Perovskites respond to strong optical absorption and consequently give high absorption coefficient. With the variation of halide (Cl to I), the absorption can be adjusted to cover the whole visible range (Figure 1.4c). Combination of halogen p-orbital and metal s-orbital form the VBM of perovskites. When switching the halide from Cl to I, their p-character increases in the VBM which in turn decreases the band gap [32]. Note that, $CsPbI_3$ has better absorption properties than the other $CsPbX_3$ perovskites, and the absorption edge is

located at 1.52 eV, signifying that $CsPbI_3$ will absorb all visible light [33]. With the change in X, optical band gap can be tuned from about 1.55 eV to 3.2 eV [16,34]

1.3.3.2. Photoluminescence (PL) response

The PeNCs can outperform their bulk counterparts in terms of luminescence, making them intriguing for a range of applications. PeNCs' PL features rely on a number of variables, some of which are listed below-

(a) Composition dependency: As already mentioned, the absorption and emission properties of PeNCs can be modified over the full visible spectra either by adjusting the composition of halide ratio in mixed halide PeNCs or exchanging the halides. Due to the high mobility of charge carriers, halide ion of perovskites can be exchanged partially or entirely with each other. With the change in anion from Cl to I the emission wavelength changes from blue to red region (Figure 1.4a & b). Perturbation of the A site cation also influences the PL features by distorting the BX_6^{4-} octahedron. A larger or smaller cation (for example, FA^+ = 0.19 –0.22 nm, Cs^+ = 0.167 nm, or Rb^+ = 0.152 nm) induces the crystal lattice to expand or contract, resulting in a change in the B-X bond length, which in turn impact the emission behavior [35,36].

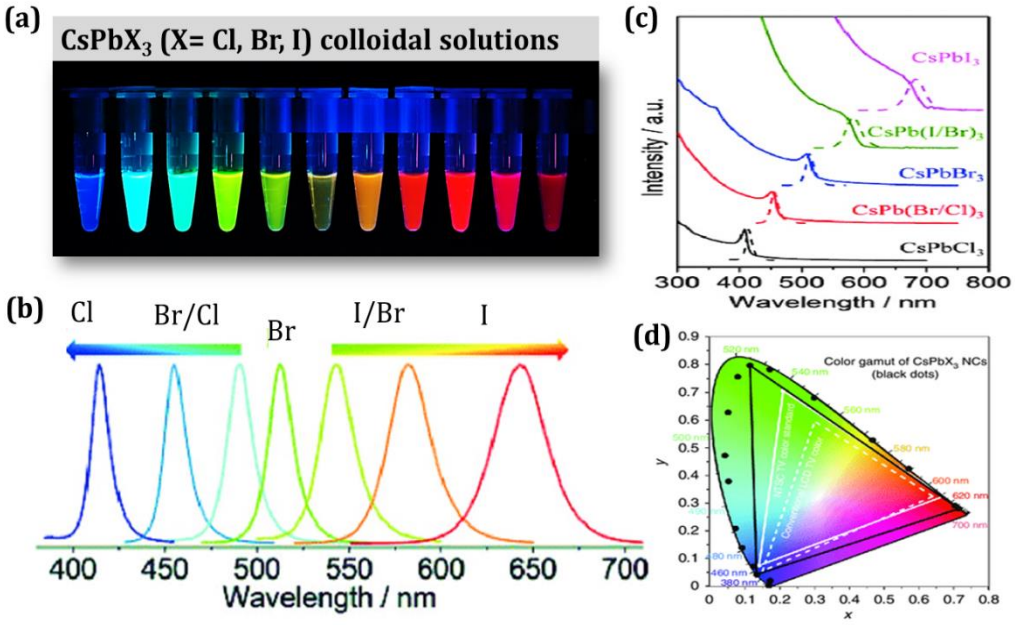

Figure 1.4: Tunable emission colors of $CsPbX_3$ colloidal NCs dispersion under UV lamp (λ = 365 nm) (a), Corresponding emission spectra under 365 nm excitation wavelength (b), absorption spectra (c), and CIE chromaticity diagram (black dots represent the emission from $CsPbX_3$ PeNCs) (d) with various halide composition of $CsPbX_3$ NCs.

(b) Temperature dependent PL: The emission characteristics of PeNCs also show temperature dependency. For $CH_3NH_3PbBr_3$ PeNCs, within 4 –120 K temperature the PL intensity first declined, then showed a slight variation from 100 K to 273 K and the loss was almost 70% PL intensity at higher temperature (300 – 400 K). Similarly, $CsPbX_3$ PeNCs showed PL quenching at higher temperature. Bulk perovskites, on the other hand exhibited an exponential reduction in PL intensity prior to about 100 K and then became nonluminescent [37,38].

(c) Defect tolerance: In comparison with the conventional QDs MHPs have high tolerance capacity to defect density. A defect state arises in PeNCs because of various structural like vacancy or surface related defects. But the defects in perovskites located in either VBM or CBM, not within the band gap, which is a very unique property of metal halide perovskite nanomaterials. In this context, PeNCs show very high PLQY without the need for any electronic surface passivating agent. However, such surface passivation is necessary to attain a high PLQY value from conventional metal chalcogenides QDs [4,39].

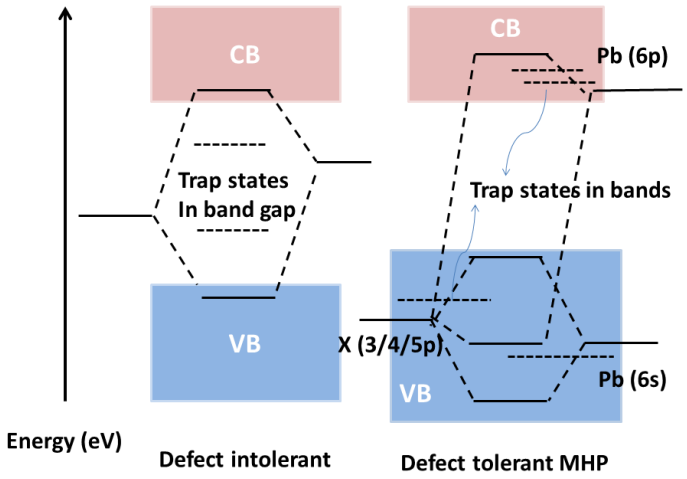

Figure 1.5: Schematic of band structure of defect intolerant semiconductor NCs and defect tolerant lead halide perovskite NCs.

(d) Quantum Confinement (Size dependent PL): Optical properties of perovskites are also controlled by the size of the perovskite crystal. Nanoscale perovskites have the ability to efficiently reduce exciton dissociation and increase radiative recombination. All the research studies revealed that the perovskite material at nanoscale acts as an efficient means of enhancing optoelectronic device performance. Quantum confinement comes into role when the size of PeNCs is below the exciton Bohr radius,

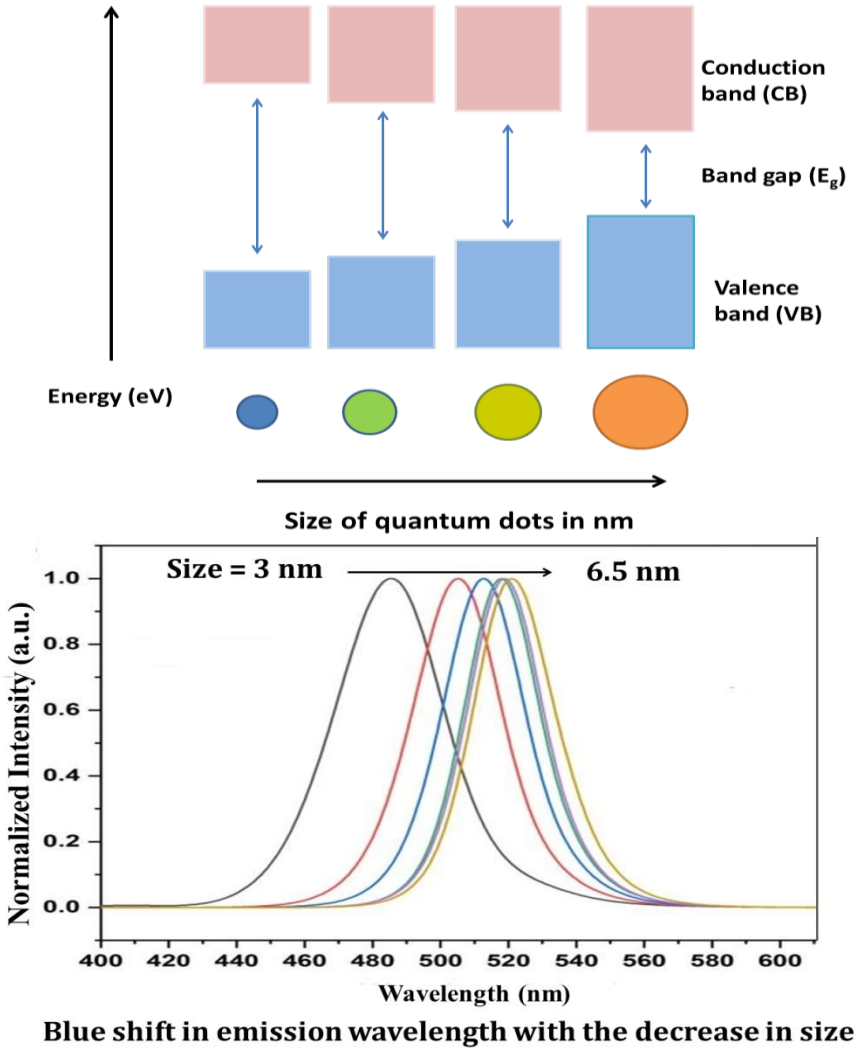

Figure 1.6: Schematic representation of size dependent band gap and blue shifted emission of $CsPbX_3$ PeNCs.

as observed by the emergence of narrow emission and excitonic peak, blue shift of absorption spectra and luminescence spectra [32]. Quantum confinement effects in $CsPbBr_3$ PeNCs are characterized by the gradual blue shift in the absorption peak with decreasing crystal size from 6.2 nm to 3.7 nm, which is associated with the blue shift of emission peaks [40] (Figure 1.6). This phenomenon was also observed in perovskite nanowires and nanoplatelets [41,42].

1.4. Materials and methods

1.4.1. $CsPbBr_3$ Perovskite: The $CsPbBr_3$ perovskite belongs to all inorganic perovskites family. The Goldschmidt tolerance factor of $CsPbBr_3$ is 0.92, which is much closer to 1 than that of $CsPbI_3$ (0.89) [43,44]. That is why $CsPbBr_3$ PeNCs have greater chemical stability than their $CsPbI_3$ counterparts. When compared to hybrid organic-inorganic

MHPs also, $CsPbBr_3$ perovskites demonstrate significantly higher thermal and chemical stability. It has a substantially higher onset decomposition temperature (~853 K) than $MAPbBr_3$ and $FAPbBr_3$ having decomposition temperatures in the range of 423-523 K [45,46]. There are often three distinct structural phases present in $CsPbBr_3$, the cubic (*Pm3m*), tetragonal (*P4/mbm*), and orthorhombic (*Pbnm*) phases [47]. They exhibit excellent optical properties. In general, it shows a highly intense and narrow green emission. The $CsPbBr_3$ could be a great material for various applications because of its simple synthesis, and superior properties. Several methods for synthesizing PeNCs are outlined below.

1.4.1.1. Synthetic strategies of perovskite nanocrystals

In recent years, simple approaches for synthesizing PeNCs of various dimensions, size and shape have arrested a lot of scientific interest. The synthesis method can be broadly classified into top down and bottom up approach. The top-down method involves the mechanical (ball-milling) or chemical (e.g., chemical exfoliation) fragmentation of macromolecules, whereas the bottom-up approach begins with molecules and ions and proceeds through gas or liquid phase chemical reactions [48]. The liquid-phase technique or wet chemical process was found to be the most effective one for the development of colloidal PeNCs (Figure 1.7) which are as discussed below –

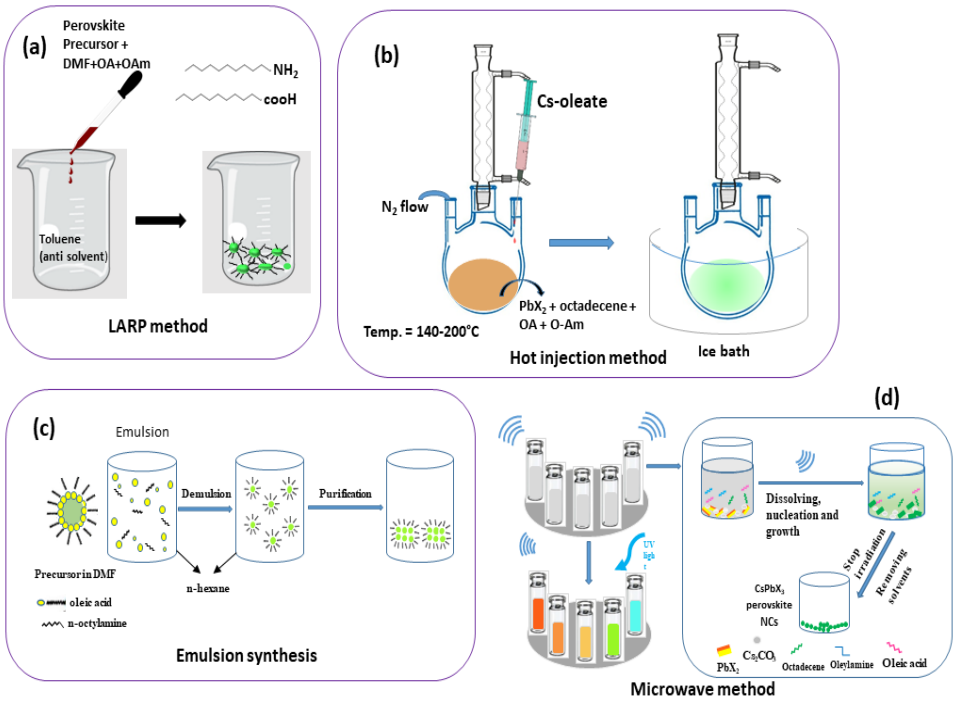

Figure 1.7: Schematic diagram of different synthetic approach of perovskite nanocrystals, (a) Ligand-assisted reprecipitation method, (b) Hot injection method, (c) Emulsion synthesis, and (d) Microwave synthesis.

(a) Hot injection method (HI)

HI or high temperature method is conventionally used for the synthesis of metal chalcogenide nanocrystals [49]. In this method, a cation precursor e.g. Cs^+ or MA^+ in oleate form is rapidly injected into a hot solution of metal halide precursor and organic ligands under inert atmosphere. Upon immediate injection, a fast nucleation occurs with the simultaneous formation of PeNCs. By achieving a separation between the nucleation and growth stages, this technique allows for the synthesis of PeNCs with a restricted size distribution. Controlling several parameters such as reaction temperature, ratio between the surfactants and precursors, precursor concentration and time of reaction, the size and shape of colloidal PeNCs can be tuned. This HI method was modified by Protesescu et al. to synthesize all inorganic cesium lead halide PeNCs by injecting Cs-oleate precursor into a PbX_2 (X= Br, Cl, I) solution containing oleyl amine (OAm), Oleic acid (OA), trioctylphosphine (TOPO), and octadecene (ODE) at high temperature (140-200°C) under an inert atmosphere [16]. A very high PLQY up to 90% was achieved for $CsPbX_3$ PeNCs by this method. Although the HI approach provides the finest morphological control in PeNCs synthesis, but its high cost makes it unsuitable for mass production due to the requirement of very high temperature and inert atmosphere. Consequently, the need for alternate synthesis methods has emerged.

(b) Ligand-assisted reprecipitation method (LARP)

The low cost LARP technique is the most often utilized approach to synthesize $CsPbBr_3$ PeNCs at room temperature. Hybrid organic-inorganic perovskite nanocrystals were first synthesized by Schmidt et al. in which 6 nm sized stable colloidal solution of $MAPbBr_3$ PeNCs with PLQY value of 20% was formed by using a long chain alkyl ammonium bromide (OABr) with OA and ODE as ligand [50]. Following this literature, LARP and emulsion synthesis have been developed. Zhang et al. introduced LARP technique to produce $MAPbX_3$ (X= Cl, Br, I) PeNCs with PLQY 50-70 % [51]. In the LARP method, perovskite precursors and ligands were dissolved in DMF (polar solvent). Then a definite volume of the precursor solution was added into toluene (non-polar anti solvent) with vigorous stirring. The antisolvent induces the crystallization of perovskite nanoparticles with bright fluorescent color due to the lowering of solubility. In order to manage the sizes and shape of PeNCs, the choice of ligands and solvents used in precursors are crucial. In the year 2016, $CsPbX_3$ PeNCs were synthesized using this method. It is possible to systematically alter the morphology of $CsPbX_3$ colloidal nanocrystals into a variety of

different shapes, including spherical quantum dots, nanocubes, nanorods, and nanoplatelets, using this simple LARP technique that can be carried out at room temperature (25 °C) [52].

(c) Emulsion synthesis

This method is divided into two basic steps; emulsion formation and demulsion. A pair of immiscible solvents e.g., DMF and n-hexane along with surfactant (OA) and the precursors of perovskites (PbX_2, CsX, CH_3NH_3X) were used to create an emulsion system. To break the emulsion, demulsifier (e.g., tert-butanol, acetone) was added. Then, the mixing of precursors could cause a change in solubility which further accelerates the nucleation and crystallization of PeNCs. This approach improves the crystallization control process of PeNCs, yielding monodisperse perovskite QDs with adjustable sizes ranging from 2 to 8 nm with absolute PLQYs of 80−92% [53].

(d) Microwave and ultrasonic method

Song et al. were the first to demonstrate ultrasound-assisted synthesis of PeNCs [54]. These methods are mainly used to produce large scale synthesis of PeNCs. A polar solvent-free synthesis approach is provided by this method. Long et al. described a microwave-assisted technique to produce high quality $CsPbX_3$ PeNCs with a controlled morphology [55]. Microwave heating provides various advantages such as reduced energy costs and high heating rates that produce uniform nano particles with excellent photo physical characteristics. Here, a heterogeneous solid–liquid reaction system of ODE, OA, OAm, PbX_2, Cs_2CO_3 was poured in a glass vessel and then put in a microwave oven. The $CsPbX_3$ PeNCs were produced using microwave irradiation for approximately 4 minutes. The size and shape of the NCs formed by this method were microwave irradiation time dependent. When the irradiation time was 2 min, irregular nanocubes of $CsPbI_3$ PeNCs with 4.9-5.3 nm size were formed. The size of the NCs increased to 11 nm when the irradiation time was increased to 7 min.

1.4.2. Metal halide perovskite (MHP) nanocomposites

Due to the ionic nature and low lattice formation energy of MHPs they suffer from poor stability, it degrades when exposed to extreme environmental conditions such as moisture, heat, and ultra-violet (UV) light. Thus, technical applications that require the PeNCs to expose in an external energy source for an extended period of time are restricted by this chemical instability. Numerous efforts have been approached to stabilize PeNCs by integrating perovskites with different classes of materials (polymer matrix, SiO_2, zeolite,

Al_2O_3, TiO_2, MOF) to produce perovskite heterostructures [56-63]. Among these conventional inorganic materials, metal organic frameworks (MOFs) have earned a significant attention due to their high porosity, functional diversity, tunable pore size, structural adjustability, and very high specific surface area [64]. It has been shown that encapsulating $CsPbX_3$ PeNCs in the MOF matrices to create host–guest composites is an easy and effective approach [65]. The strong host–guest interactions and the MOFs' substantial surface area, stabilize the nano confined guest species without the need for additional stabilizing agents [66, 67]. Figure 1.8 illustrated the various scientific efforts towards the stabilization of $CsPbX_3$ perovskites.

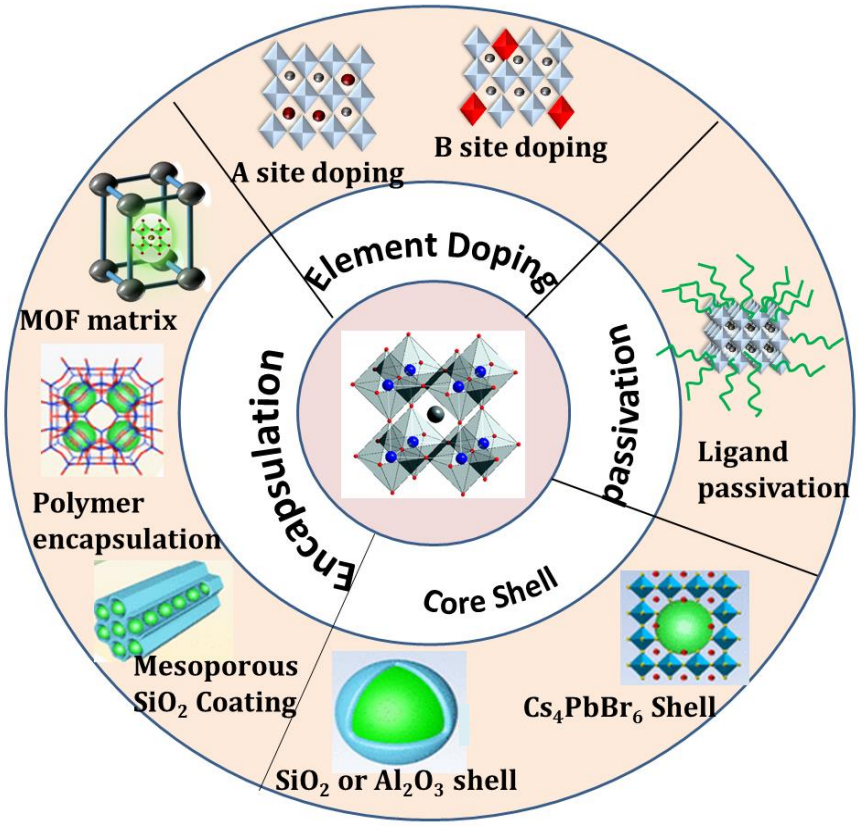

Figure 1.8: Different stabilization methods of halide perovskite materials.

1.4.3. Metal organic framework (MOF)

MOFs belong to the family of those hybrid porous materials which are crystalline in nature and are composed by virtue of the integration of several organic linkers and inorganic metal ion cluster. Generally, the former (organic linkers) are di, tri, or tetra-dentate ligand whereas the inorganic components are typically isolated polyhedral or small cluster unit [68].

Synthesis method of MOF: Numerous MOFs with various metal centers and linkers have been developed so far for a variety of functions. Table 1.1 illustrates some examples of different MOFs with their method of synthesis. The most common synthesis techniques of MOFs include conventional solvothermal method, diffusion, microwave assisted, electrochemical, mechanochemical, and sonochemical methods (Table 1.1).

Table 1.1 Summary of synthesis techniques followed for different MOFs with their building units

Synthesis Method	Synthesized MOF	Solvent	Metal node	Organic Linker	Ref
Solvothermal Method	MOF-5	DMF	$Zn(NO_3)_2 \cdot 6H_2O$	1,4-Benzene dicarboxylic acid (H_2BDC)	[69]
	UIO-66, UIO-67	DMF, H_2O	$ZrCl_4$	H_2BDC,4,4′-biphenyl dicarboxylate	[70,71]
	MIL-101	H_2O	$Cr(NO_3)_3 \cdot 9H_2O$	H_2BDC	[72]
	MIL-125	DMF/ CH_3OH	Titanium butoxide	H_2BDC	[73,74]
	PCN-221	DEF	$ZrCl_4$	4-carboxyphenyl porphyrin	[75]
Microwave synthesis	Ni-MOF-74	DMF, CH_3OH, water	$Ni(NO_3)_2 \cdot 6H_2O$	2,5-dihydroxyterephthalic acid	[76]
	Ca-BDC	DMF	$Ca(NO_3)_2.4H_2O$	H_2BDC	[77]
	ZIF-8	DMF	$Zn(NO_3)_2 \cdot 6H_2O$	2-Methyl imidazole	[78]
	MOF-5, IRMOF-2, and 3	DEF	$Zn(NO_3)_2 \cdot 6H_2O$	H_2BDC	[79]

Electrochemical Synthesis	Cu-BTC	CH_3OH	Cu-Plate	1,3,5-Benzentricarboxylic acid (BTC)	[80]
	ZIF-8	Water	Zn wire	2-methylimidazole	[81]
	HKUST-1	Ethanol	Cu sphere	BTC	[81]
	MIL-100 (Al)	Water/ Ethanol	Al electrode	benzene tricarboxylate	[82]
Sonochemical Synthesis	MOF 5	NMP	$Zn(NO_3)_2.6H_2O$	H_2BDC	[83]
	MOF-177	NMP	$Zn(NO_3)_2.6H_2O$	4,4′,4″-benzene-1,3,5-triyl-tribenzoic acid	[84]
Mechanochemical Synthesis	MOF-74	Solvent free	$Mg(NO_3)_2 \cdot 6H_2O$	2,5-dihydroxyterephthalic acid	[85]
	HKUST-1(Cu-BTC)	Solvent free	$Cu(OAc)_2.H_2O$	1,3,5-benzenetricarboxylate	[86]

1.4.4. MHP/MOF hybrid nanocomposites

As mentioned earlier, the environmental stabilization of luminescent perovskite nanocrystals is an unresolved scientific problem. As an approach towards the improvement of the stability of them, PeNCs are incorporated in porous MOF matrix to produce perovskite/MOF nano hybrid. In the following section, we have discussed the formation process of PeNCs in the MOF matrix.

1.4.4.1. Synthesis method of MHP/MOF hybrid

Several strategies have been established to generate high quality Perovskite MOF composite with confined size, advanced optical and electrical features. Here, we use four different categories outlined in this section to summarize the synthesis procedure for Perovskite MOF heterostructures (Figure 1.9)

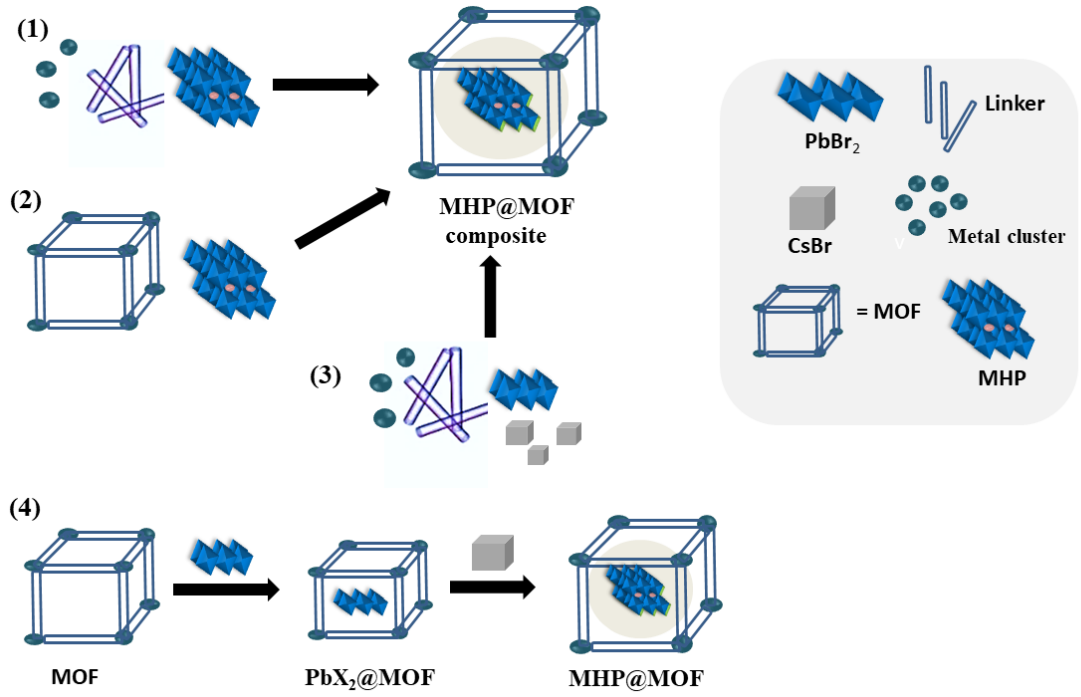

Figure 1.9: Schematic representations of different synthetic methods of perovskite/MOF heterostructures.

(a) Bottle around ship technique: In this process, MOFs are assembled on templates made from pre-synthesized perovskites. This involves single step loading of pre-formed PeNCs into the building units of MOF precursors. Pre-synthesized luminescent PeNCs are mixed with the MOF precursors, which are then allowed to react under the same reaction conditions as those used to create pristine MOFs. Su et al. in 2018 used this process to encapsulate $CsPbX_3$ in the zeolitic imidazole framework (ZIF-8 and ZIF-67) by forming a coating layer of zeolitic imidazole framework around the $CsPbX_3$ PeNCs. Previously synthesized $CsPbBr_3$ QDs were dispersed in precursor solutions of metal ions and an imidazole linker to generate MOF coating layer on the surface of PeQDs [87].

(b) Ship in a bottle technique: This strategy enables the encapsulation of PeNCs to the pre-formed MOF cavities that offers adaptable sites and size for the nucleation of PeNCs. The resulting perovskite MOF composite was formed either through a straightforward mixing procedure of pre-made MHPs and MOFs, or by adding perovskite precursors into MOFs during its formation [88]. This mixing method prevents interference between MOF and PeNCs synthesis, enabling PeNC-MOF composites formation with fluorescence and crystallinity remain intact. However, pore size of the MOF must be considered, as MOFs having bigger pores in general can aid in the postsynthetic incorporation of perovskites to the MOF. Wang and his team in the year 2019 synthesized a stable $CsPbX_3$/MOF-5 hybrid

involving the use of a MOF-5 crystal to grow the perovskites. They adjusted the pore structure of MOF-5 by controlling the composition ratio of CTAB and TMB as template molecule and obtained the resulting $CsPbX_3$/MOF-5 composite by physical mixing of the solution of PeNCs with mesoporous MOF [89].

(c) One step in situ method: This technique simultaneously develops MOF crystals and PeNCs. Typically, both the precursors of MOF and perovskites are mixed together and the reaction conditions are controlled to form the perovskite in the MOF matrix [90]. After that, anti-solvent is introduced to nucleate the PeNCs into the MOF matrix and finally produce the perovskite MOF nanocomposites. The "one-step" synthetic strategy requires less time, solvent, and energy, making this methodology more efficient and environmentally friendly. However, because the conditions used for the synthesis of MOFs and perovskites are typically different, this "one-step" method requires additional research in the future [91].

(d) Two step in situ conversion procedure: The first step of this process involves either the formation of Pb-MOF lattice with Pb as metal cluster or the incorporation of lead halide to the MOF matrix to form PbX_2@MOF. In the next step, Pb-MOF is converted to perovskite by the interaction with CsX or MAX salt. Perovskite nanocrystals can grow spontaneously in ambient settings, or they can be stimulated by temperature changes or the addition of antisolvents [92]. Zhang and his team in 2015 reported a hybrid Cu-BTC thin film, where $MAPbI_2X$ PeNCs were incorporated by a sequential two step deposition process [93]. The pre made Cu-BTC film was first soaked in PbX_{-2} solution to form PbX_2@HKUST-1 thin film. Then, $MAPbI_2X$ perovskite QDs were entrapped inside the MOF by treating PbX_2@HKUST-1 film with the ethanolic solution of MAX to finally create the $MAPbI_2X$@Cu-BTC hybrid film. In 2017, Zhang et al. utilized the similar two-step process to convert an invisible Pb-MOF to luminescent $MAPbBr_3$ MOF composite in powder form [94].

1.5. Applications of Perovskite based composite materials

Gradually, human dependency is shifting towards the use of flexible optoelectronic devices such as display devices, solar cell, computing devices, sensors, and memory devices. This shift in human dependency can be attributed to their advantageous features. The advantageous nature of optoelectronic devices has escalated solely due to the use of perovskites. These perovskites are used in many optoelectronic applications like solar cells, LED, photodetectors, lasers, field effect transistors etc. Of late, the applications of

perovskites are not only restricted in the field of devices but also as sensor materials due to their excellent optical, electrical and sensing properties. Herein, we shall briefly discuss about the use of perovskite halides in solar cells and LED but the thrust area will be on the use of MHPs as optically active sensor material.

1.5.1. Optoelectronic Devices

Light Emitting Diode (LED): Highly luminescent perovskite quantum dots have impressive properties such as very high PLQY, color purity, tunability of emission colors, and high external quantum efficiency (EQE). Researchers now a day utilize blue, green, and red emission of lead halide PeNCs for the fabrication of various perovskite LEDs. The broad color selectivity of $CsPbX_3$ PeQDs allows a high color rendering index and an appropriate correlated color temperature, even accommodating the most visible part of sunlight with minimal UV and blue emission, resulting in healthy lighting [95–97]. Such optical qualities offer them great potential in lighting and displays. Song and his groups in 2015 first reported $CsPbX_3$ perovskite QDs based LED with EQE value of 0.07%, 0.12%, and 0.09% for blue, green and white colored LEDs [98]. However, the poor stability of the PeNCs in ambient environment greatly limits their application in LEDs. Therefore. Perovskite-LEDs made from MOF-based perovskite nanocomposites are gaining popularity in recent years due to their stable emission performance and processing simplicity [89, 99-104].

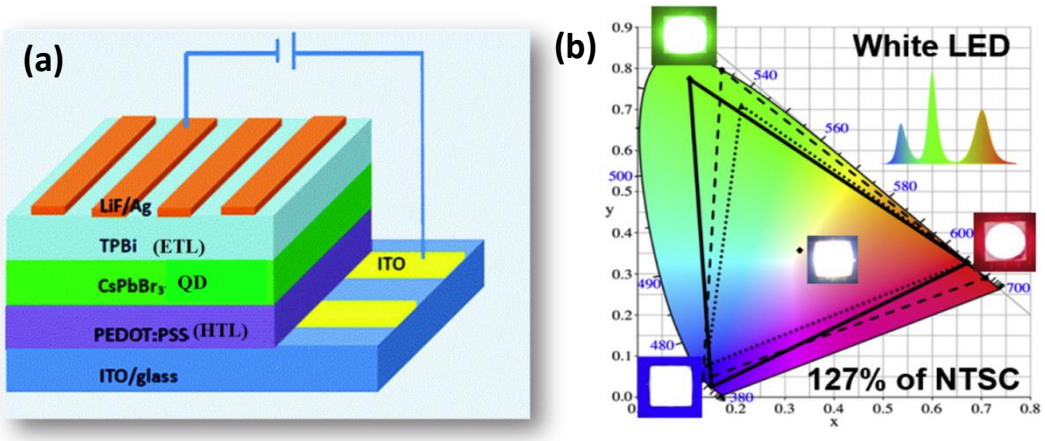

Figure 1.10: Device structure of a LED (a), CIE color coordinates of white LED of $CsPbBr_3$ PeNCs (b) [105].

1.5.2. Photovoltaic applications

A revolution of thin film solar cells has been sparked by metal-halide perovskite materials since the breakthrough in 2009 by Kojima's team [15] with 3.9 % efficiency. Since then,

the efficiency of perovskite photovoltaic has been reached over 25% within few years [106,107]. Similarly, MHP quantum dots have recently become a promising material in QD based perovskite solar cells. In the year of 2016, NREL scientists for the first time reported $CsPbI_3$ QD solar cell where cesium cation replaces the organic part of the $MAPbI_3$ and achieved better stability than organometal halide perovskite solar cells with 10% PCE [108]. Figure 1.11 demonstrated the device structure of perovskite solar cell (FTO/ETM/Perovskite/HTM/Ag). The device structure of a perovskite solar cell composed of an electron transport layer, perovskite absorber as light harvesting material, and a hole transport layer. It has either conventional n-i-p structure or inverted p-i-n configuration. Researchers are currently focused on enhancing the stability of perovskite solar cells through a variety of methods such as doping, interfacial layer modification, passivation, encapsulation method etc. [25, 109].

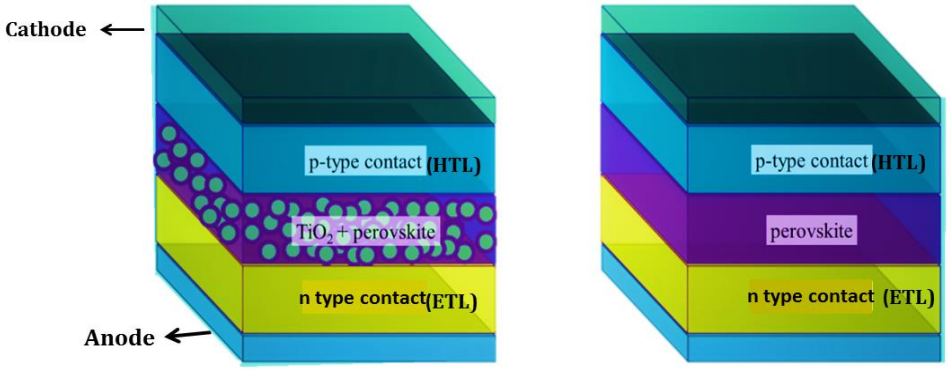

Figure 1.11: Device architecture of two types of perovskites solar cells.

1.5.3. As Sensor materials

After achieving extraordinary success in optoelectronic devices, PeNCs are very recently applied in the field of sensing benefitting from their outstanding optical and electrical properties. This thesis report mainly focuses on the sensing applications of perovskite materials. Systems that transform the chemical signals into a useful analytical signal are termed as chemical sensors. A specific interaction between a sensing material in the sensor and a target analyte produces the signal due to the changes in physical properties of the sensing probe. Chemical sensors can further be classified into optical and electrochemical sensor on the basis of detection method used for analyte. When exposed to an external stimulus, the physical parameters of metal halide perovskites such as absorbance, PL emission intensity and wavelength, as well as electrical characteristics are modified.

Therefore, the perovskite nanomaterials can be employed as both optical and electrochemical sensing material based on the technique used for the detection of target molecules.

1.5.3.1. Electrical Sensor

Several electrochemical sensing techniques e.g., anodic stripping voltammetric method (ASV), photo-electrochemistry (PEC), electrochemiluminescence (ECL), and chemiresistance (CR) have been widely used for the detection of analytes via electrochemical method [110]. Mostly oxide perovskites (e.g., strontium and lanthanide based perovskite oxides) have been frequently utilized as ASV sensor for wide range of chemicals and biomolecules as they offer high electrical conductivity, catalytic activity, stability, oxide mobility within the crystal, and electrically active structure [111]. PEC sensing method stands out as an analytical method for transforming chemical energy into a photocurrent signal in the presence of light. Accordingly, high-performance MHPs are considered among the effective PEC materials for PEC sensing applications. Recently, a water resistant $CsPbBr_3$/rGO nanoscroll composite has been synthesized by Chen and his group toward stable PEC sensing of mycotoxins, aflatoxin B1 or ochratoxin A [112]. The multilayer of rGO provide strong interfacial contacts with $CsPbBr_3$ QDs and embed the QDs in rGO nanosheets to prevent them from external environment. The band alignment and rapid surface carrier transport further boost the anodic photocurrent responsiveness for PEC sensing. Perovskite QDs are also a good candidate for ECL sensing applications. Zou's team in 2016 first reported $CsPbBr_3$ PeNCs as ECL emitter [113]. Huang's group in the next year developed $CsPbBr_3$ PeNCs modified glassy carbon electrode as an ECL sensor for H_2O_2 detection [114]. Recently, wang and his coworkers synthesized a stable MOF encapsulated $CH_3NH_3PbBr_3$ QDs for the recognition of aflatoxin B1 in corn samples [115]. Moisture sensitive nature of MHPs enables them to utilize in humidity sensing. In 2015, Hu and his group used CR method in solution processed $CH_3NH_3PbI_{3-x}Cl_x$ film for humidity sensing application [116]. On exposure of relative humidity from 32% to 97%, the electrical resistance of the perovskite films varied from 98% to 25% of its initial value. Similar CR method was reported in several literatures for the detection of gas molecules [117,118].

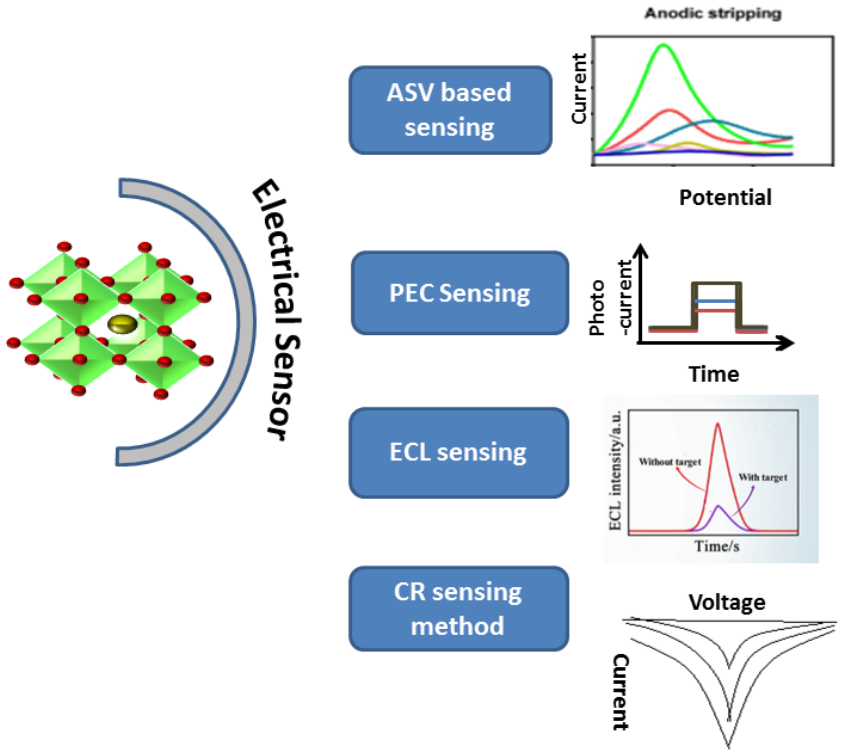

Figure 1.12: Diagram showing the different electrical sensing methods using MHPs.

1.5.3.2. Optical Sensor

The optical sensor measures the change in optical parameter related to the analyte concentration. It is usually made up of a chemical recognition system (called a "receptor") and a transducer. The transducer transforms the signal from the receptor into a quantifiable signal that can be processed via amplification, filtering, recording and so on. The receptor interacts with target analytes and recognizes variables like pH, analyte concentration and so on. It generates an optical signal proportional to the magnitude of these parameters. The principle of optical sensing is mainly based on light absorption and emission. In light emission or luminescence based sensing methods, the target analyte interacts with the PeNCs surface and changes the emission peak of the perovskites (either quenching or enhancement of the FL signal). They have advantage over light absorption method because of its excellent selectivity and sensitivity (thousand times greater than absorption based method) [119]. In luminescence based quenching method, the decrease in intensity can be discussed using the Stern- volmer relation:

$$F_o/F = 1+K_{SV}[C] \qquad (1.3)$$

where F_o and F represent the PL emission intensities of the fluorophore before and after the addition of the analyte respectively, $[C]$ is the concentration of analyte and K_{SV} is the Stern –Volmer quenching constant which indicates the sensitivity of receptor molecule to

the quencher. PeNCs with their great optical properties can act as an intriguing candidate for optical sensor materials. Static and dynamic quenching are the two basic divisions in optical sensing mechanism. The effects of dynamic quenching are further categorized into- i) FRET (Forster resonance energy transfer), ii) electron transfer, iii) Inner filter effect (IFE), and so forth [120]. By taking into account the PeNCs, we have emphasized the mechanism responsible for the sensing of diverse analytes.

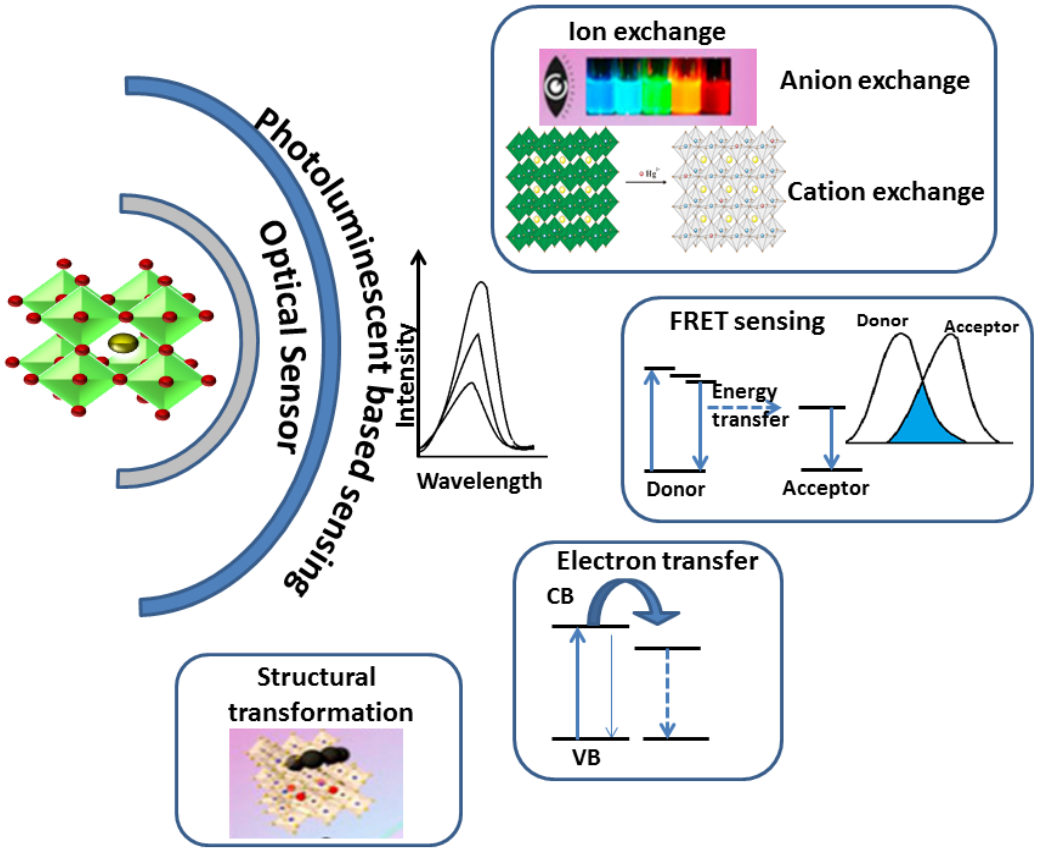

Figure 1.13: MHPs as optical sensor and its different optical sensing steps.

(a) Static quenching

In static quenching, the fluorophores form a nonfluorescent ground state complex with quenchers. It does not depend on diffusion or molecular collisions. The absorption or emission spectra of the fluorophore are either shifted or changed after the introduction of target analyte in static quenching [120]. In case of PeNCs this can be best understood through ion exchange mechanism. Moreover, on exposure to gases e.g., amine vapors and NH_3 gas molecules reversible H-bonding interaction between perovskites and the gas molecules takes place, leading to a change in optical properties of PeNCs. Also, the gas molecules can intercalate into the perovskite crystal lattices to form an intermediate

complex which can revert back to perovskite before the irreversible decomposition of PeNCs. This reversible nature greatly enhances the reproducibility of perovskite based sensing systems [121,122].

Ion exchange: In ABX_3 type MHPs, the composition can be tuned by adjusting the B site cation and the X anions, which can further change the emission property such as wavelength shift or quenching of emission peak of PeNCs. Based on these cation and anion exchange principles of perovskite material, several works of metal sensing (both cations and anions) have been reported. MHPs have very fast anion exchange property in presence of different halide salts which can cause emission wavelength shift of PeNCs, covering the whole visible spectrum. This is an ideal property for colorimetric sensing and many researchers utilize this property for visual detection applications [123]. Park and his team used $CsPbBr_3$/cellulose based nano composite for colorimetric detection of Cl^- & I^- in tap water [124]. The porous cellulose fibers facilitated the strong attachment of $CsPbBr_3$ and thereby improved the PL stability of the composite. The colorimetric sensing ability of this nano composite was mainly based on the anion exchange property of lead halide perovskites. The sensing probe showed a fast response with the introduction of Cl^- and I^- with the shift in PL peak. Similarly, B site cation exchange with the analyte molecule also takes place which tunes the composition of PeNCs resulting in a change in fluorescence intensity [125,126]. Analytical methods such as XPS, EDX and XRD further give the evidence of ion exchange mechanism of PeNCs in presence of sensing elements.

(b) Dynamic quenching

Dynamic quenching takes place when the interaction between the fluorophore and the quencher occurs via encounters that are diffusive in nature. Since it affects the donor's excited states only, it has no discernible influence on the absorption spectra.

i) FRET (Forster Resonance Energy Transfer): When the donor and acceptor moieties are separated by a distance of 15 Å to 100 Å, the emission spectra of the donor and the absorption spectrum of the acceptor overlap [120]. The energy transfer occurs as a result of this activity is termed as FRET. In this process, the donor and the acceptor are connected by a dipole-dipole interaction. Energy transfer depends on donor-acceptor distance and the extent of spectral overlap. A $CsPbBr_3$/PMMA fiber membrane designed using electro-spinning method was employed as a FRET based fluorescence detector for metal ions, biological proteins and pH sensing. After attaching cyclam with Cu^{2+}, FRET process occurs between $CsPbBr_3$ and cyclam–Cu^{2+} leading to the quenching of fluorescence and

detect Cu^{2+} with LOD (Limit of detection) 10^{-15} M [127]. Wang et al. used polystyrene fiber matrix to prepare $CsPbBr_3$-PS nanocomposites via electrospinning process. A great overlap between the emission of $CsPbBr_3$-PS and the absorption spectrum of rhodamine 6G enable the composite to act as FRET probe for detection of R6G [128].

ii) Electron transfer: In addition to the compositional changes, the efficient charge separation and exciton diffusion in perovskite nanomaterials enable electron transfer from perovskite to the electron deficient analyte upon exposure to external stimulation. When the valence band and conduction band energy levels of perovskites are aligned with acceptor moieties, electron transfer occurs between the sensing probe and the analyte molecule. Accordingly, the PL signal of the perovskites quenches by electron transfer from the excited state of perovskite to the quencher. This property of PeNCs has been used for the sensing of various metal ions, toxic gases, explosives, biomolecules etc. [129-131]. Chen et al. reported $CsPbBr_3$ and $CsPbI_3$ PeNCs, as a fluorescent sensor for selective discrimination of picric acid (PA) against other nitroaromatic explosives. They suggested electrostatic interaction assisted electron transfer between PeNCs and PA with the help of UV-visible spectroscopy, XPS analysis, and density functional theory (DFT) calculations. DFT calculation provides that the LUMO energy level of strong electrophilic PA (E_{LUMO} = −3.897 eV) is lower than that of $CsPbBr_3$ (E_{LUMO} = −3.6 eV) and $CsPbI_3$ (E_{LUMO} = −3.75 eV), signifying the feasibility of excited electrons transferred from the PeQDs to PA and resulting fluorescence quenching [131]. Another research work employed $CsPbBr_3$ PeQDs for Cu^{2+}metal ion sensing in organic phase with LOD value of 0.1 nM. They explained the PL quenching phenomenon on the basis of electron transfer from PeQDs to Cu^{2+} and the process was confirmed by the photoluminescence decay life time measurements [129]. Huang and Tong group further used this photo induced charge transfer assisted luminescence quenching process of $CsPbBr_3$ PeNCs for the detection of omethoate insecticide and tetracycline antibiotic [130].

iii) Defect induced PL sensing: PeNCs can adsorb small molecules or ions on their surface, which induces new surface defect states for non-radiative recombination pathways resulting in the decrease of PL intensity. Sheng and his research team reported colloidal $CsPbBr_3$ PeNCs for the detection of Cu^{2+} in non-polar medium, various bio oils and industrial oils [132]. The LOD was found to be 2 nM with high sensitivity, selectivity and rapid response. DFT calculations reveal that in the VBM edge of $CsPbBr_3$ QD, the Cu^{2+} addition resulted in the emergence of various new states or defect levels due to the formation of Br-Cu-OOCH complex on the surface of PeNCs. After the excitation of

PeNCs, the hole created in the HOMO of the perovskite is filled by these new states that facilitates nonradiative pathways for electron/hole recombination and finally quench the FL signal of $CsPbBr_3$. In addition to the crystal size and structure, the surface smoothness also plays a pivotal role in the selective detection of metal ions.

Shan et al. reported a stable porous nanocomposites consisting of $MAPbBr_3$ nanocrystals embedded in a poly (vinylidene fluoride) (PVDF) polymer matrix for the selective detection of 2,4,6 -trinitrotoluene (TNT) vapor [133]. After exposure to the TNT vapor, strong quenching of PL signal was observed which was mainly due to the introduction of more defect levels in the PeNCs. Transient absorption spectroscopy (TAS) analysis results displayed reduced carrier lifetime of $MAPbBr_3$/PVDF composite in presence of TNT further validate this assumption.

(c) Perovskites as humidity and temperature sensor

Furthermore, the instability of PeNCs on exposure to humidity can alter the photoluminescence property of perovskites [134,135]. This property is reversible under controlled conditions. A reversible phase transformation of perovskites generally occurs with a change in temperature, which can be reflected in their PL spectrum. Therefore, PeNCs can be used as suitable fluorescent temperature and humidity sensor [122,136]. The $MAPbBr_3$ was utilized as humidity sensor which was synthesized by a simple grinding of $PbBr_2$ and MABr in 20% relative humidity. With the increase of humidity within the range of 7-98%, the PL intensity at 530 nm was quenched gradually due to instability of PeNCs in presence of moisture. The process was reversible when the interaction of $MAPbBr_3$ with water molecule was for a short time period [134].

1.6. Objectives

The emerging trend in perovskite based material research revealed from their diverse applications owing to their outstanding optical and electrical properties mentioned in the previous sections. However, the main obstacle to the PeNCs lies in the degradation of the material under ambient environmental conditions such as moisture, heat, UV light, polar solvents, etc. Very recently researchers have directed their efforts to utilizing the luminescent properties and sensitive nature of MHPs in the area of sensing. Despite the huge potential of using pristine MHPs as sensors, improving the water resistivity and long-term stability in real, complex environments remains one of the major challenges. Because of stability issue, most of the sensing applications using $CsPbX_3$ PeQDs are limited to non-polar media, which makes it difficult for real detection applications.

In this concern, many research studies have been conducted to stabilize the perovskite nano materials. Porous matrix for instance MOF material with very high surface area makes them a great host material for PeNCs. Integrating the PeNCs with MOFs can create a protective shield against external environment. Employing MOF for the preparation of stable perovskite nano hybrid is a recent strategy that achieves superior optical properties along with prolonged lifetimes. Considering the state of art literature at the moment, very few research works have been carried out highlighting synthesis of perovskite/MOF (Pe-MOF) nano hybrid and and even fewer of those exploited fluorescence sensing applications. Hence, motivated from the improved luminescence properties of stable Pe-MOF nano hybrid, their sensing abilities can be explored for various target analytes in ambient environment. In light of these considerations, the following objectives have been established for the current study.

1. To synthesize $CsPbX_3$/Zn-HIMDC, $CsPbBr_3$/ZIF-8, $CsPbBr_3$/HZIF-8, $CsPbBr_3$/Eu-BDC metal halide perovskite-MOF hybrid composites.
2. To study structural, morphological, and optical characterization of the synthesized materials using various spectroscopic and analytical techniques.
3. To explore luminescence properties of Perovskite-MOF nanocomposites and stability test of the composites over bare $CsPbX_3$ PeNCs.
4. To optimize the performance of the prepared Perovskite-MOF composites and utilize them as stable optical sensing probe for various analytes detection.

1.7. Plan of research & thesis outlook

To accomplish the proposed objectives, the research work was organized as follows-

1) Extensive literature survey has been carried out on perovskite based materials
2) Synthesis of MOFs and Perovskite/MOF nanocomposites was considered employing different routes. They mostly include-
    - Solvothermal synthesis and simple room temperature reaction method using metal source and linker for MOF synthesis.
    - One step or two step in situ room temperature surfactant free growth of $CsPbX_3$ QDs in the MOF matrix.
3) Characterization of the perovskite/MOF composites: All the synthesized compounds are characterized using various analytical techniques e.g. Fourier transform infrared (FTIR) spectroscopy, X-ray diffraction (XRD), X-ray

photoelectron spectroscopy (XPS), UV-visible absorption spectrophotometer, fluorescence spectrophotometer, Time-resolved Photoluminescence Spectroscopy (TRPL), scanning electron microscopy (SEM), transmission electron microscopy (TEM), and energy dispersive X-ray (EDX) spectrometry, BET analysis etc.

4) Luminescence responses and Stability of the synthesized perovskite/MOF composite are studied in ambient atmospheric conditions.
5) The optimal conditions for employing synthesized $CsPbBr_3$/MOF composites as an efficient optical sensor towards various analytes are also determined.
6) Study of the sensing performance using Stern-Volmer plot and selectivity study of the sensing probe are also worked out.
7) The sensing performances are also assessed out for use in real sample analysis.

1.8. References

[1] Parida, B., Ryu, J., Yoon, S., Lee, S., Seo, Y., Cho, J. S., and Kang, D. W. Two-step growth of CsPbI 3− X Br X films employing dynamic CsBr treatment: Toward all-inorganic perovskite photovoltaics with enhanced stability. *Journal of Materials Chemistry A*, 7(31):18488-18498, 2019.

[2] Wang, X., He, J., Mao, L., Cai, X., Sun, C., and Zhu, M. CsPbBr3 perovskite nanocrystals anchoring on monolayer MoS2 nanosheets for efficient photocatalytic CO2 reduction. *Chemical Engineering Journal*, 416:128077, 2021.

[3] Zhang, C., Wang, S., Li, X., Yuan, M., Turyanska, L., and Yang, X. Core/shell perovskite nanocrystals: synthesis of highly efficient and environmentally stable FAPbBr3/CsPbBr3 for LED applications. *Advanced Functional Materials*, 30(31):1910582, 2020.

[4] Huang, H., Bodnarchuk, M. I., Kershaw, S. V., Kovalenko, M. V., and Rogach, A. L. Lead halide perovskite nanocrystals in the research spotlight: stability and defect tolerance. *ACS energy letters*, 2(9):2071-2083, 2017.

[5] Zhao, Y., Xu, Y., Shi, L., and Fan, Y. Perovskite nanomaterial-engineered multiplex-mode fluorescence sensing of edible oil quality. *Analytical chemistry*, 93(31):11033-11042, 2021.

[6] Huangfu, C. and Feng, L. High-performance fluorescent sensor based on CsPbBr3 quantum dots for rapid analysis of total polar materials in edible oils. *Sensors and Actuators B: Chemical*, 344:130193, 2021.

[7] Lemanov, V., Sotnikov, A., Smirnova, E., Weihnacht, M., and Kunze, R. Perovskite CaTiO3 as an incipient ferroelectric. *Solid State Communications*, 110(11): 611-614, 1999.

[8] He, J., Liu, Y., and Funahashi, R. Oxide thermoelectrics: The challenges, progress, and outlook. *Journal of Materials Research*, 26(15): 1762-1772, 2011.

[9] Rubel, M. H., Takei, T., Kumada, N., Ali, M. M., Miura, A., Tadanaga, K., Oka, K., Azuma, M., Yashima, M., and Fujii, K. Hydrothermal synthesis, crystal structure, and superconductivity of a double-perovskite Bi oxide. *Chemistry of Materials*, 28(2): 459-465, 2016.

[10] Wollan, E. and Koehler, W. Neutron diffraction study of the magnetic properties of the series of perovskite-type Compounds [(1− x) La, x Ca] Mn O 3. *Physical Review*, 100(2): 545, 1955.

[11] Møller, C. K. Crystal structure and photoconductivity of caesium plumbohalides. *Nature*, 182(4647):1436-1436, 1958.

[12] Wells, H. L. Über die cäsium-und kalium-bleihalogenide. *Zeitschrift für anorganische Chemie*, 3(1):195-210, 1893.

[13] Sahoo, S. K., Manoharan, B., and Sivakumar, N. *Introduction: Why perovskite and perovskite solar cells?*, Perovskite photovoltaics. Academic Press, 1-24, 2018.

[14] Weber, D. CH3NH3PbX3, ein Pb (II)-system mit kubischer perowskitstruktur/CH3NH3PbX3, a Pb (II)-system with cubic perovskite structure. *Zeitschrift für Naturforschung B*, 33(12):1443-1445, 1978.

[15] Kojima, A., Teshima, K., Shirai, Y., and Miyasaka, T. Organometal halide perovskites as visible-light sensitizers for photovoltaic cells. *Journal of the american chemical society*, 131(17):6050-6051, 2009.

[16] Protesescu, L., Yakunin, S., Bodnarchuk, M. I., Krieg, F., Caputo, R., Hendon, C. H., Yang, R. X., Walsh, A. and Kovalenko, M. V. Nanocrystals of cesium lead halide perovskites (CsPbX3, X= Cl, Br, and I): novel optoelectronic materials showing bright emission with wide color gamut. *Nano letters*, 15(6):3692-3696, 2015.

[17] Gao, P., Grätzel, M., and Nazeeruddin, M. K. Organohalide lead perovskites for photovoltaic applications. *Energy & Environmental Science*, 7(8):2448-2463, 2014.

[18] Zhai, X., Ding, F., Zhao, Z., Santomauro, A., Luo, F., and Tong, J. Predicting the formation of fractionally doped perovskite oxides by a function-confined machine learning method. *Communications Materials*, 3(1):42, 2022.

[19] Song, J., Li, J., Li, X., Xu, L., Dong, Y., and Zeng, H. Quantum dot light-emitting diodes based on inorganic perovskite cesium lead halides (CsPbX3). *Advanced materials*, 27(44):7162-7167, 2015.

[20] Mahesh, K. P. O., Chang, C. Y., Hong, W. L., Wen, T. H., Lo, P. H., Chiu, H. Z., Hsu, C. L., Horng, S. F. and Chao, Y. C., Lead-free cesium tin halide nanocrystals for light-emitting diodes and color down conversion. *RSC advances*, 10(61):37161-37167, 2020.

[21] Kagan, C. R., Mitzi, D. B., and Dimitrakopoulos, C. D. Organic-inorganic hybrid materials as semiconducting channels in thin-film field-effect transistors. *Science*, 286(5441):945-947, 1999.

[22] Luo, S. and Daoud, W. A. Recent progress in organic–inorganic halide perovskite solar cells: mechanisms and material design. *Journal of Materials Chemistry A*, 3(17):8992-9010, 2015.

[23] Li, M., Li, H., Fu, J., Liang, T., and Ma, W. Recent progress on the stability of perovskite solar cells in a humid environment. *The Journal of Physical Chemistry C*, 124(50):27251-27266, 2020.

[24] Green, M. A., Ho-Baillie, A., and Snaith, H. J. The emergence of perovskite solar cells. *Nature photonics*, 8(7):506-514, 2014.

[25] Parida, B., Yoon, S., Jeong, S. M., Cho, J. S., Kim, J. K., and Kang, D. W. Recent progress on cesium lead/tin halide-based inorganic perovskites for stable and efficient solar cells: A review. *Solar Energy Materials and Solar Cells*, 204:110212, 2020.

[26] Saparov, B., and Mitzi, D. B. Organic–inorganic perovskites: structural versatility for functional materials design. *Chemical reviews*, 116(7):4558-4596, 2016.

[27] Lufaso, M. W. and Woodward, P. M. Jahn–Teller distortions, cation ordering and octahedral tilting in perovskites. *Acta Crystallographica Section B: Structural Science*, 60(1):10-20, 2004.

[28] Chang, Y., Park, C. H., and Matsuishi, K. First-principles study of the Structural and the electronic properties of the lead-Halide-based inorganic-organic perovskites (CH3NH3) PbX3 and CsPbX3 (X= Cl, Br, I). *Journal-Korean Physical Society*, 44: 889-893, 2004.

[29] Chen, Q., De Marco, N., Yang, Y. M., Song, T. B., Chen, C. C., Zhao, H., Hong, Z., Zhou, H., and Yang, Y. Under the spotlight: The organic–inorganic hybrid halide perovskite for optoelectronic applications. *Nano Today*, 10(3):355-396, 2015.

[30] Kang, J. and Wang, L. W. High defect tolerance in lead halide perovskite CsPbBr3. *The journal of physical chemistry letters*, 8(2):489-493, 2017.

[31] Swarnkar, A., Chulliyil, R., Ravi, V. K., Irfanullah, M., Chowdhury, A., and Nag, A. Colloidal CsPbBr3 perovskite nanocrystals: luminescence beyond traditional quantum dots. *Angewandte Chemie*, 127(51):15644-15648, 2015.

[32] Chouhan, L., Ghimire, S., Subrahmanyam, C., Miyasaka, T., and Biju, V. Synthesis, optoelectronic properties and applications of halide perovskites. *Chemical Society Reviews*, 49(10):2869-2885, 2020.

[33] Chen, H., Li, M., Wang, B., Ming, S., and Su, J. Structure, electronic and optical properties of CsPbX3 halide perovskite: a first-principles study. *Journal of Alloys and Compounds*, 862:158442, 2021.

[34] Yang, Z., Surrente, A., Galkowski, K., Miyata, A., Portugall, O., Sutton, R. J., Haghighirad, A. A., Snaith, H. J., Maude, D. K., Plochocka, P., and Nicholas, R. J. Impact of the halide cage on the electronic properties of fully inorganic cesium lead halide perovskites. *ACS Energy letters*, 2(7):1621-1627, 2017.

[35] Luis, K., Ono, E. J., and Juarez-Perez, Y. Progress on novel perovskite materials and solar cells with mixed cations and halide anions. *ACS Applied Materials & Interfaces*, 9(36):30197-30246, 2017.

[36] Amat, A., Mosconi, E., Ronca, E., Quarti, C., Umari, P., Nazeeruddin, M. K., Gratzel, M., and De Angelis, F. Cation-induced band-gap tuning in organohalide perovskites: interplay of spin–orbit coupling and octahedra tilting. *Nano letters*, 14(6):3608-3616, 2014.

[37] Deng, W., Fang, H., Jin, X., Zhang, X., Zhang, X., and Jie, J. Organic–inorganic hybrid perovskite quantum dots for light-emitting diodes. *Journal of Materials Chemistry C*, 6(18):4831-4841, 2018.

[38] Milot, R. L., Eperon, G. E., Snaith, H. J., Johnston, M. B. and Herz, L. M. Temperature-dependent charge-carrier dynamics in CH3NH3PbI3 perovskite thin films. *Advanced Functional Materials*, 25(39):6218-6227, 2015.

[39] Dirin, D. N., Protesescu, L., Trummer, D., Kochetygov, I. V., Yakunin, S., Krumeich, F., Stadie, N. P., and Kovalenko, M. V. Harnessing defect-tolerance at

the nanoscale: highly luminescent lead halide perovskite nanocrystals in mesoporous silica matrixes. *Nano letters*, 16(9):5866-5874, 2016.

[40] Dong, Y., Qiao, T., Kim, D., Parobek, D., Rossi, D., and Son, D. H. Precise control of quantum confinement in cesium lead halide perovskite quantum dots via thermodynamic equilibrium. *Nano letters*, 18(6):3716-3722, 2018.

[41] Akkerman, Q. A., Motti, S. G., Srimath Kandada, A. R., Mosconi, E., D'Innocenzo, V., Bertoni, G., and Manna, L. Solution synthesis approach to colloidal cesium lead halide perovskite nanoplatelets with monolayer-level thickness control. *Journal of the American Chemical Society*, 138(3):1010-1016, 2016.

[42] Zhang, D., Yu, Y., Bekenstein, Y., Wong, A. B., Alivisatos, A. P., and Yang, P. Ultrathin colloidal cesium lead halide perovskite nanowires. *Journal of the American Chemical Society*, 138(40):13155-13158, 2016.

[43] Zhang, Y., Siegler, T. D., Thomas, C. J., Abney, M. K., Shah, T., De Gorostiza, A., Greene, R. M., and Korgel, B. A. A "tips and tricks" practical guide to the synthesis of metal halide perovskite nanocrystals. *Chemistry of Materials*, 32(13):5410-5423, 2020.

[44] Travis, W., Glover, E. N. K., Bronstein, H., Scanlon, D. O., Palgrave, R. G. On the Application of the Tolerance Factor to Inorganic and Hybrid Halide Perovskites: A Revised System. *Chem. Sci.* 7:4548−4556, 2016.

[45] Kulbak, M., Gupta, S., Kedem, N., Levine, I., Bendikov, T., Hodes, G., and Cahen, D. Cesium enhances long-term stability of lead bromide perovskite-based solar cells. *The journal of physical chemistry letters*, 7(1):167-172, 2016.

[46] Hanusch, F. C., Wiesenmayer, E., Mankel, E., Binek, A., Angloher, P., Fraunhofer, C., Giesbrecht, N., Feckl, J. M., Jaegermann, W., Johrendt, D., and Bein, T., Efficient planar heterojunction perovskite solar cells based on formamidinium lead bromide. *The journal of physical chemistry letters*, 5(16): 2791-2795, 2014.

[47] Yang, D. and Huo, D. Cation doping and strain engineering of CsPbBr 3-based perovskite light emitting diodes. *Journal of Materials Chemistry C*, 8(20):6640-6653, 2020.

[48] Wang, S., Yousefi Amin, A. A., Wu, L., Cao, M., Zhang, Q., and Ameri, T. Perovskite Nanocrystals: Synthesis, Stability, and Optoelectronic Applications. *Small Structures*, 2(3):2000124, 2021.

[49] Murray, C., Norris, D. J., and Bawendi, M. G. Synthesis and characterization of nearly monodisperse CdE (E= sulfur, selenium, tellurium) semiconductor

nanocrystallites. *Journal of the American Chemical Society*, 115(19):8706-8715, 1993.

[50] Schmidt, L. C., Pertegás, A., González-Carrero, S., Malinkiewicz, O., Agouram, S., Minguez Espallargas, G., Bolink, H. J., Galian, R. E., and Pérez-Prieto, J., Nontemplate synthesis of CH3NH3PbBr3 perovskite nanoparticles. *Journal of the American Chemical Society*, 136(3):850-853, 2014.

[51] Zhang, F., Zhong, H., Chen, C., Wu, X. G., Hu, X., Huang, H., Han, J., Zou, B., and Dong, Y. Brightly luminescent and color-tunable colloidal CH3NH3PbX3 (X= Br, I, Cl) quantum dots: potential alternatives for display technology. *ACS nano*, 9(4):4533-4542, 2015.

[52] Sun, S., Yuan, D., Xu, Y., Wang, A., and Deng, Z., Ligand-mediated synthesis of shape-controlled cesium lead halide perovskite nanocrystals via reprecipitation process at room temperature. *ACS nano*, 10(3):3648-3657, 2016.

[53] Huang, H., Zhao, F., Liu, L., Zhang, F., Wu, X. G., Shi, L., Zou, B., Pei, Q., and Zhong, H., Emulsion synthesis of size-tunable CH3NH3PbBr3 quantum dots: an alternative route toward efficient light-emitting diodes. *ACS applied materials & interfaces*, 7(51):28128-28133, 2015.

[54] Jang, D. M., Kim, D. H., Park, K., Park, J., Lee, J. W., and Song, J. K. Ultrasound synthesis of lead halide perovskite nanocrystals. *Journal of Materials Chemistry C*, 4(45):10625-10629, 2016.

[55] Long, Z., Ren, H., Sun, J., Ouyang, J., and Na, N. High-throughput and tunable synthesis of colloidal CsPbX 3 perovskite nanocrystals in a heterogeneous system by microwave irradiation. *Chemical Communications*, 53(71):9914-9917, 2017.

[56] Li, M., Li, H., Fu, J., Liang, T., and Ma, W. Recent progress on the stability of perovskite solar cells in a humid environment. *The Journal of Physical Chemistry C*, 124(50):27251-27266, 2020.

[57] Sun, J. Y., Rabouw, F. T., Yang, X. F., Huang, X. Y., Jing, X. P., Ye, S., and Zhang, Q. Y. Facile two-step synthesis of all-inorganic perovskite CsPbX3 (X= Cl, Br, and I) zeolite-Y composite phosphors for potential backlight display application. *Advanced Functional Materials*, 27(45):1704371, 2017.

[58] Li, B., Zhang, Y., Fu, L., Yu, T., Zhou, S., Zhang, L., and Yin, L. Surface passivation engineering strategy to fully-inorganic cubic CsPbI3 perovskites for high-performance solar cells. *Nature communications*, 9(1):1076, 2018.

[59] Zhou, Q., Bai, Z., Lu, W. G., Wang, Y., Zou, B., and Zhong, H. In situ fabrication of halide perovskite nanocrystal-embedded polymer composite fims with enhanced photoluminescence for display backlights, *Adv. Mater.* 28:9163–9168, 2016.

[60] Wang, H. C., Lin, S. Y., Tang, A. C., Singh, B. P., Tong, H. C., Chen, C. Y., Lee, Y. C., Tsai, T. L., and Liu, R. S. Mesoporous silica particles integrated with all-inorganic CsPbBr3 perovskite quantum-dot nanocomposites (MP-PQDs) with high stability and wide color gamut used for backlight display. *Angewandte Chemie International Edition*, 55(28):7924-7929, 2016.

[61] Li, Z. J., Hofman, E., Li, J., Davis, A. H., Tung, C. H., Wu, L. Z., and Zheng, W. Photoelectrochemically active and environmentally stable CsPbBr3/TiO2 core/shell nanocrystals. *Advanced Functional Materials*, 28(1):1704288, 2018.

[62] Li, Z., Kong, L., Huang, S., and Li, L. Highly luminescent and ultrastable CsPbBr3 perovskite quantum dots incorporated into a silica/alumina monolith. *Angewandte Chemie*, 129(28):8246-8250, 2017.

[63] Rambabu, D., Bhattacharyya, S., Singh, T., ML, C., and Maji, T. K. Stabilization of MAPbBr3 perovskite quantum dots on perovskite MOFs by a one-step mechanochemical synthesis. *Inorganic chemistry*, 59(2):1436-1443, 2020.

[64] Shen, K., Zhang, L., Chen, X., Liu, L., Zhang, D., Han, Y., Chen, J., Long, J., Luque, R., Li, Y. and Chen, B. Ordered macro-microporous metal-organic framework single crystals. *Science*, 359(6372):206-210, 2018.

[65] Nie, W. and Tsai, H. Perovskite nanocrystals stabilized in metal–organic frameworks for light emission devices. *Journal of Materials Chemistry A*, 10(37):19518-19533, 2022.

[66] Cuan, J., Zhang, D., Xing, W., Han, J., Zhou, H., and Zhou, Y. Confining CsPbX3 perovskites in a hierarchically porous MOF as efficient and stable phosphors for white LED. *Chemical Engineering Journal*, 425:131556, 2021.

[67] Bhattacharyya, S., Rambabu, D., and Maji, T. K. Mechanochemical synthesis of a processable halide perovskite quantum dot–MOF composite by post-synthetic metalation. *Journal of Materials Chemistry A*, 7(37):21106-21111, 2019.

[68] Stock, N. and Biswas, S. Synthesis of metal-organic frameworks (MOFs): routes to various MOF topologies, morphologies, and composites. *Chemical reviews*, 112(2):933-969, 2012.

[69] McKinstry, C., Cathcart, R. J., Cussen, E. J., Fletcher, A. J., Patwardhan, S. V., and Sefcik, J. Scalable continuous solvothermal synthesis of metal organic framework (MOF-5) crystals. *Chemical Engineering Journal*, 285:718-725, 2016.

[70] Valenzano, L., Civalleri, B., Chavan, S., Bordiga, S., Nilsen, M. H., Jakobsen, S., Lillerud, K. P., and Lamberti, C. Disclosing the complex structure of UiO-66 metal organic framework: a synergic combination of experiment and theory. *Chemistry of Materials*, 23(7):1700-1718, 2011.

[71] Arrozi, U. S., Wijaya, H. W., Patah, A., and Permana, Y. Efficient acetalization of benzaldehydes using UiO-66 and UiO-67: Substrates accessibility or Lewis acidity of zirconium. *Applied Catalysis A: General*, 506:77-84, 2015.

[72] Férey, G., Mellot-Draznieks, C., Serre, C., Millange, F., Dutour, J., Surblé, S., and Margiolaki, I. A chromium terephthalate-based solid with unusually large pore volumes and surface area. *Science*, 309(5743):2040-2042, 2005.

[73] Dan-Hardi, M., Serre, C., Frot, T., Rozes, L., Maurin, G., Sanchez, C., and Férey, G. A new photoactive crystalline highly porous titanium (IV) dicarboxylate. *Journal of the American Chemical Society*, 131(31):10857-10859, 2009.

[74] Chi, W. S., Roh, D. K., Lee, C. S., and Kim, J. H. A shape-and morphology-controlled metal organic framework template for high-efficiency solid-state dye-sensitized solar cells. *Journal of Materials Chemistry A*, 3(43):21599-21608, 2015.

[75] Wu, L. Y., Mu, Y. F., Guo, X. X., Zhang, W., Zhang, Z. M., Zhang, M., and Lu, T. B. Encapsulating perovskite quantum dots in iron-based metal–organic frameworks (MOFs) for efficient photocatalytic CO2 reduction. *Angewandte Chemie International Edition*, 58(28):9491-9495, 2019.

[76] Chen, C., Feng, X., Zhu, Q., Dong, R., Yang, R., Cheng, Y., and He, C. Microwave-assisted rapid synthesis of well-shaped MOF-74 (Ni) for CO2 efficient capture. *Inorganic chemistry*, 58(4):2717-2728, 2019.

[77] George, P., Das, R. K., and Chowdhury, P. Facile microwave synthesis of Ca-BDC metal organic framework for adsorption and controlled release of Curcumin. *Microporous and Mesoporous Materials*, 281:161-171, 2019.

[78] Van Tran, T., Nguyen, H., Le, P. H. A., Nguyen, D. T. C., Nguyen, T. T., Van Nguyen, C., Vo, D. V. N., and Nguyen, T. D. Microwave-assisted solvothermal fabrication of hybrid zeolitic–imidazolate framework (ZIF-8) for optimizing dyes

adsorption efficiency using response surface methodology. *Journal of Environmental Chemical Engineering*, 8(4):104189, 2020.

[79] Ni, Z. and Masel, R. I. Rapid production of metal− organic frameworks via microwave-assisted solvothermal synthesis. *Journal of the American Chemical Society*, 128(38):12394-12395, 2006.

[80] Mueller, U., Schubert, M., Teich, F., Puetter, H., Schierle-Arndt, K., and Pastre, J. Metal–organic frameworks—prospective industrial applications. *Journal of Materials Chemistry*, 16(7):626-636, 2006.

[81] Yadnum, S., Roche, J., Lebraud, E., Négrier, P., Garrigue, P., Bradshaw, D., and Kuhn, A. Site-selective synthesis of janus-type metal-organic framework composites. *Angewandte Chemie*, 126(15):4082-4086, 2014.

[82] Martinez Joaristi, A., Juan-Alcañiz, J., Serra-Crespo, P., Kapteijn, F., and Gascon, J. Electrochemical synthesis of some archetypical Zn2+, Cu2+, and Al3+ metal organic frameworks. *Crystal Growth & Design*, 12(7):3489-3498, 2012.

[83] Son, W. J., Kim, J., Kim, J., and Ahn, W. S. Sonochemical synthesis of MOF-5. *Chemical Communications*, (47):6336-6338, 2008.

[84] Jung, D. W., Yang, D. A., Kim, J., Kim, J., and Ahn, W. S. Facile synthesis of MOF-177 by a sonochemical method using 1-methyl-2-pyrrolidinone as a solvent. *Dalton Transactions*, 39(11):2883-2887, 2010.

[85] Wang, Z., Li, Z., Ng, M., and Milner, P. J. Rapid mechanochemical synthesis of metal–organic frameworks using exogenous organic base. *Dalton Transactions*, 49(45):16238-16244, 2020.

[86] Yuan, W., Garay, A. L., Pichon, A., Clowes, R., Wood, C. D., Cooper, A. I., and James, S. L. Study of the mechanochemical formation and resulting properties of an archetypal MOF: Cu3 (BTC) 2 (BTC= 1, 3, 5-benzenetricarboxylate). *CrystEngComm*, 12(12):4063-4065, 2010.

[87] Kong, Z. C., Liao, J. F., Dong, Y. J., Xu, Y. F., Chen, H. Y., Kuang, D. B., and Su, C. Y. Core@ shell CsPbBr3@ zeolitic imidazolate framework nanocomposite for efficient photocatalytic CO2 reduction. *ACS Energy Letters*, 3(11):2656-2662, 2018.

[88] Hou, J., Wang, Z., Chen, P., Chen, V., Cheetham, A. K., and Wang, L. Intermarriage of halide perovskites and metal-organic framework crystals. *Angewandte Chemie*, 132(44):19602-19617, 2020.

[89] Ren, J., Li, T., Zhou, X., Dong, X., Shorokhov, A. V., Semenov, M. B., Krevchik, V. D., and Wang, Y. Encapsulating all-inorganic perovskite quantum dots into mesoporous metal organic frameworks with significantly enhanced stability for optoelectronic applications. *Chemical Engineering Journal*, 358:30-39, 2019.

[90] Mollick, S., Mandal, T. N., Jana, A., Fajal, S., Desai, A. V., and Ghosh, S. K. Ultrastable luminescent hybrid bromide perovskite@ MOF nanocomposites for the degradation of organic pollutants in water. *ACS Applied Nano Materials*, 2(3):1333-1340, 2019.

[91] Li, B., Suo, T., Xie, S., Xia, A., Ma, Y. J., Huang, H., Zhang, X., and Hu, Q. Rational design, synthesis, and applications of carbon dots@ metal–organic frameworks (CD@ MOF) based sensors. *TrAC Trends in Analytical Chemistry*, 135:116163, 2021.

[92] Tsai, H., Shrestha, S., Vilá, R. A., Huang, W., Liu, C., Hou, C. H., and Nie, W. Bright and stable light-emitting diodes made with perovskite nanocrystals stabilized in metal–organic frameworks. *Nature Photonics*, 15(11):843-849, 2021.

[93] Chen, Z., Gu, Z. G., Fu, W. Q., Wang, F., and Zhang, J. A confined fabrication of perovskite quantum dots in oriented MOF thin film. *ACS applied materials & interfaces*, 8(42):28737-28742, 2016.

[94] Zhang, C., Wang, B., Li, W., Huang, S., Kong, L., Li, Z., and Li, L., Conversion of invisible metal-organic frameworks to luminescent perovskite nanocrystals for confidential information encryption and decryption. *Nature communications*, 8(1):1138, 2017.

[95] Pradhan, N. Journey of making cesium lead halide perovskite nanocrystals: what's next, *J. Phys. Chem. Lett*. 10:5847–5855, 2019.

[96] Li, X. , Wu, Y., Zhang, S., Cai, B., Gu, Y., J. Song, and Zeng, H. CsPbX3 quantum dots for lighting and displays: room-temperature synthesis, photoluminescence superiorities, underlying origins and white light-emitting diodes, *Adv. Funct. Mater*. 26:2435–2445, 2016.

[97] Zhao, F., Song, Z., Zhao, J., and Liu, Q. Double perovskite Cs 2 AgInCl 6: Cr 3+: broadband and near-infrared luminescent materials. *Inorganic Chemistry Frontiers*, 6(12):3621-3628, 2019.

[98] Song, J., Li, J., Li, X., Xu, L., Dong, Y., and Zeng, H. Quantum dot light-emitting diodes based on inorganic perovskite cesium lead halides (CsPbX3). *Advanced materials*, 27(44):7162-7167, 2015.

[99] Mollick, S., Mandal, T. N., Jana, A., Fajal, S., and Ghosh, S. K. A hybrid blue perovskite@ metal–organic gel (MOG) nanocomposite: simultaneous improvement of luminescence and stability. *Chemical Science*, 10(45):10524-10530, 2019.

[100] Ren, J., Zhou, X., and Wang, Y. Dual-emitting CsPbX3@ ZJU-28 (X= Cl, Br, I) composites with enhanced stability and unique optical properties for multifunctional applications. *Chemical Engineering Journal*, 391:123622, 2020.

[101] Zhang, D., Zhao, J., Liu, Q., and Xia, Z. Synthesis and luminescence properties of CsPbX3@ Uio-67 composites toward stable photoluminescence convertors. *Inorganic Chemistry*, 58(2):1690-1696, 2019.

[102] Zhao, Y., Xie, C., Zhang, X., and Yang, P. CsPbX3 quantum dots embedded in zeolitic imidazolate framework-8 microparticles for bright white light-emitting devices. *ACS Applied Nano Materials*, 4(5):5478-5485, 2021.

[103] Zhang, Q., Wu, H., Lin, W., Wang, J., and Chi, Y. Enhancing air-stability of CH3NH3PbBr3 perovskite quantum dots by in-situ growth in metal-organic frameworks and their applications in light emitting diodes. *Journal of Solid State Chemistry*, 272:221-226, 2019.

[104] Tsai, H., Huang, H. H., Watt, J., Hou, C. H., Strzalka, J., Shyue, J. J., Wang, L., and Nie, W. Cesium Lead Halide Perovskite Nanocrystals Assembled in Metal-Organic Frameworks for Stable Blue Light Emitting Diodes. *Advanced Science*, 9(14):2105850, 2022.

[105] Park, D. H., Han, J. S., Kim, W., and Jang, H. S. Facile synthesis of thermally stable CsPbBr3 perovskite quantum dot-inorganic SiO2 composites and their application to white light-emitting diodes with wide color gamut. *Dyes and Pigments*, 149:246-252, 2018.

[106] Yang, W. S., Noh, J. H., Jeon, N. J., Kim, Y. C., Ryu, S., Seo, J., and Seok, S. I., High-performance photovoltaic perovskite layers fabricated through intramolecular exchange. *Science*, 348(6240):1234-1237, 2015.

[107] Ding, B., Li, Y., Huang, S. Y., Chu, Q. Q., Li, C. X., Li, C. J., and Yang, G. J., Material nucleation/growth competition tuning towards highly reproducible planar

perovskite solar cells with efficiency exceeding 20%. *Journal of Materials Chemistry A*, 5(15):6840-6848, 2017.

[108] Swarnkar, A., Marshall, A. R., Sanehira, E. M., Chernomordik, B. D., Moore, D. T., Christians, J. A., and Luther, J. M. Quantum dot–induced phase stabilization of α-CsPbI3 perovskite for high-efficiency photovoltaics. *Science*, 354(6308):92-95, 2016.

[109] Zhou, H., Liang, L., Guo, Z., and Fan, R. Anti-corrosion Strategy to improve the stability of perovskite solar cells. *Nanoscale*, 2023.

[110] Baranwal, J., Barse, B., Gatto, G., Broncova, G., and Kumar, A. Electrochemical sensors, and their applications: a review. *Chemosensors*, 10(9):363, 2022.

[111] Halali, V. V., Sanjayan, C. G., Suvina, V., Sakar, M., and Balakrishna, R. G. Perovskite nanomaterials as optical and electrochemical sensors. *Inorganic Chemistry Frontiers*, 7(14):2702-2725, 2020.

[112] Mao, L., Xiao, Y., Liu, H., Zhang, X., Wang, S., Huang, W. H., and Chen, M. M. Water-Stable CsPbBr3/Reduced Graphene Oxide Nanoscrolls for High-Performance Photoelectrochemical Sensing. *Advanced Functional Materials*, 2213814, 2023.

[113] Huang, Y., Fang, M., Zou, G., Zhang, B., and Wang, H. Monochromatic and electrochemically switchable electrochemiluminescence of perovskite CsPbBr 3 nanocrystals. *Nanoscale*, 8(44): 18734-18739, 2016.

[114] Huang, Y., Long, X., Shen, D., Zou, G., Zhang, B., and Wang, H. Hydrogen peroxide involved anodic charge transfer and electrochemiluminescence of all-inorganic halide perovskite CsPbBr3 nanocrystals in an aqueous medium, *Inorg. Chem.* 56:10135-10138, 2017.

[115] Wang, Q., Xiong, C., Li, J., Deng, Q., Zhang, X., Wang, S., and Chen, M. M. High-performance electrochemiluminescence sensors based on ultra-stable perovskite quantum dots@ ZIF-8 composites for aflatoxin B1 monitoring in corn samples. *Food Chemistry*, 410:135325, 2023.

[116] Hu, L., Shao, G., Jiang, T., Li, D., Lv, X., Wang, H., and Liu, H. Investigation of the interaction between perovskite films with moisture via in situ electrical

resistance measurement. *ACS applied materials & interfaces*, 7(45):25113-25120, 2015.

[117] Zhuang, Y., Yuan, W., Qian, L., Chen, S., and Shi, G. High-performance gas sensors based on a thiocyanate ion-doped organometal halide perovskite. *Physical Chemistry Chemical Physics*, 19(20):12876-12881, 2017.

[118] Bao, C., Yang, J., Zhu, W., Zhou, X., Gao, H., Li, F., and Zou, Z. A resistance change effect in perovskite CH 3 NH 3 PbI 3 films induced by ammonia. *Chemical Communications*, 51(84):15426-15429, 2015.

[119] Lobnik, A., Turel, M., and Urek, S. K. Optical chemical sensors: design and applications. *Advances in chemical sensors*, 3-28, 2012.

[120] Lakowicz, J.R. *Principles of fluorescence spectroscopy*. Boston, MA: springer US, 3rd edition, 2006. .

[121] Zhao, Y. and Zhu, K. Optical bleaching of perovskite (CH 3 NH 3) PbI 3 through room-temperature phase transformation induced by ammonia. *Chemical Communications*, 50(13):1605-1607, 2014.

[122] Zhu, Z., Sun, Q., Zhang, Z., Dai, J., Xing, G., Li, S., Huang, X., and Huang, W. Metal halide perovskites: stability and sensing-ability. *Journal of Materials Chemistry C*, 6(38):10121-10137, 2018.

[123] Chen, X., Hu, H., Xia, Z., Gao, W., Gou, W., Qu, Y., and Ma, Y. CsPbBr 3 perovskite nanocrystals as highly selective and sensitive spectrochemical probes for gaseous HCl detection. Journal of Materials Chemistry C, 5(2):309-313, 2017.

[124] Park, B., Kang, S. M., Lee, G. W., Kwak, C. H., Rethinasabapathy, M., and Huh, Y. S. Fabrication of CsPbBr3 Perovskite Quantum Dots/Cellulose-based Colorimetric Sensor: Dual-Responsive On-site Detection of Chloride and Iodide Ions. *Industrial & Engineering Chemistry Research*, 59(2):793-801, 2019.

[125] Lu, L. Q., Tan, T., Tian, X. K., Li, Y., and Deng, P. Visual and sensitive fluorescent sensing for ultratrace mercury ions by perovskite quantum dots. *Analytica chimica acta*, 986:109-114, 2017.

[126] Aamir, M., Sher, M., Malik, M. A., Akhtar, J., and Revaprasadu, N. A chemodosimetric approach for the selective detection of Pb2+ions using a cesium based perovskite, *New J. Chem.* , 40(11):9719–9724, 2016.

[127] Wang, Y., Zhu, Y., Huang, J., Cai, J., Zhu, J., Yang, X., Shen, J., and Li, C. Perovskite quantum dots encapsulated in electrospun fiber membranes as multifunctional supersensitive sensors for biomolecules, metal ions and pH. *Nanoscale Horizons*, 2(4):225-232, 2017.

[128] Wang, Y., Zhu, Y., Huang, J., Cai, J., Zhu, J., Yang, X., Shen, J., Jiang, H., and Li, C. CsPbBr3 perovskite quantum dots-based monolithic electrospun fiber membrane as an ultrastable and ultrasensitive fluorescent sensor in aqueous medium. *The journal of physical chemistry letters*, 7(21):4253-4258, 2016.

[129] Liu, Y., Tang, X., Zhu, T., Deng, M., Ikechukwu, I. P., Huang, W., Yin, G., Bai, Y., Qu, D., Huang, X., and Qiu, F. All-inorganic CsPbBr 3 perovskite quantum dots as a photoluminescent probe for ultrasensitive Cu 2+ detection. *Journal of Materials Chemistry C*, 6(17):4793-4799, 2018.

[130] Huang, S., Guo, M., Tan, J., Geng, Y., Wu, J., Tang, Y., Su, C., Lin, C. C., and Liang, Y. Novel fluorescence sensor based on all-inorganic perovskite quantum dots coated with molecularly imprinted polymers for highly selective and sensitive detection of omethoate. *ACS applied materials & interfaces*, 10(45):39056-39063, 2018.

[131] Chen, X., Sun, C., Liu, Y., Yu, L., Zhang, K., Asiri, A. M., Marwani, H. M., Tan, H., Ai, Y., Wang, X., and Wang, S. All-inorganic perovskite quantum dots CsPbX3 (Br/I) for highly sensitive and selective detection of explosive picric acid. *Chemical Engineering Journal*, 379:122360, 2020.

[132] Sheng, X., Liu, Y., Wang, Y., Li, Y., Wang, X., Wang, X., Dai, Z., Bao, J., and Xu, X. Cesium lead halide perovskite quantum dots as a photoluminescence probe for metal ions. *Advanced Materials*, 29(37):1700150, 2017.

[133] Shan, X., Zhang, S., Zhou, M., Geske, T., Davis, M., Hao, A., Wang, H., and Yu, Z. Porous halide perovskite–polymer nanocomposites for explosive detection with a high sensitivity. *Advanced materials interfaces*, 6(3):1801686, 2019.

[134] Xu, W., Li, F., Cai, Z., Wang, Y., Luo, F., and Chen, X. An ultrasensitive and reversible fluorescence sensor of humidity using perovskite $CH_3NH_3PbBr_3$. *Journal of Materials Chemistry C*, 4(41):9651-9655, 2016.

[135] Xiang, X., Ouyang, H., Li, J., and Fu, Z. Humidity-sensitive CsPbBr3 perovskite based photoluminescent sensor for detecting Water content in herbal medicines. *Sensors and Actuators B: Chemical*, 346:130547, 2021.

[136] Liu, J., Zhao, Y., Li, X., Wu, J., Han, Y., Zhang, X., and Xu, Y. Dual-emissive CsPbBr3@ Eu-BTC composite for self-calibrating temperature sensing application. *Crystal Growth & Design*, 20(1):454-459, 2019.